Oxidation of Metals, Vol. 2, No. 1, 1970

High-Temperature Oxidation of Alloys

Graham C. Wood*

Received November 11, 1969

Some recent developments in the understanding of the oxidation of alloys at elevated temperatures are reviewed, with special reference to binary and ternary alloys upon which many commercial materials are based. Following an initial classification of alloy systems, certain basic principles and their limitations are considered, including factors determining whether an alloy displays surface scaling only, internal oxidation only, or both phenomena; the mode of distribution of cations in an oxide solid solution growing on an alloy; and doping and the Wagner–Hauffe rules. Previous alloy oxidation theory has concerned itself principally with steady-state oxidation but, in practice, behavior of the oxidizing sample in approaching the steady state, both upon initial exposure to the environment and after scale spalling induced isothermally or during thermal cycling, is often as important. Such behavior is illustrated in terms of scale establishment and with respect to compositional changes in the subjacent alloy, the importance of certain alloy and oxide properties being emphasized. After further brief consideration of steady-state scaling, the causes and consequences of breakaway oxidation are presented. The role of major and minor concentrations of third elements on scaling behavior is discussed. The paper concludes with brief reference to situations not considered in detail and with aspects requiring further study.

INTRODUCTION

Many aspects of alloy oxidation at high temperature have been well covered from several differing viewpoints in the oxidation monographs.[1–5] Because of limitations of time and space, it is not our intention to cover equally all aspects of the subject here, but rather to present selectively recent contributions to the understanding of certain binary and ternary systems, upon

*Corrosion Science Division, Department of Chemical Engineering, University of Manchester Institute of Science and Technology, Manchester, England.

which so many commercial high-temperature materials are based. Many of the examples used to illustrate concepts are drawn from the work of the author's own group. Equally, the reference list cannot be fully comprehensive; other lists of papers contributed in this area are available in recent reviews.[6,7]

Alloy components have different affinities for oxygen and do not diffuse at the same rate in the oxide or the alloy. Consequently, the simple kinetic rate equations are often not followed and the scale and alloy compositions change in a complex way with time. The second component may enter the scale, affecting its lattice defect structure, or may accumulate as metal or as oxide beneath the main scale. Also, if oxygen diffuses into the alloy in atomic form, precipitation of the oxide of the less noble metal may occur as internal oxide. When it is considered that scales can crack, contain voids, spall, sinter, and give multiple layers of irregular thickness, it is clear that the general situation is complex. It is important to attempt to break alloy oxidation down into certain limiting cases, applicable specifically to binary alloys but in a more general way to commercial alloys, which can be treated quantitatively or at least semiquantitatively.

It has become progressively clearer during the past decade that an integrated, multidiscipline approach to oxidation studies produces the most complete answer.[6] Usually about six techniques of quite different types can be managed reasonably in any research. In the type of work now being discussed, this usually involves assessment of the overall reaction rate by kinetic measurements, study of the morphology, structure, and composition of the oxide and alloy by chemical and physical techniques, the isolation or identification of the rate-determining layer, and finally study of its defect structure and influence on the mechanical properties of the sample.

Thermodynamics, usually in the form of ternary equilibrium diagrams involving two alloying components and oxygen (or sulfur, etc.), are useful in predicting the alloying element likely to be preferentially oxidized and sometimes the likely steady-state scale. They can also provide information on subsequent reactions, such as the changes occurring when internal oxide is incorporated into the main scale. The application of thermodynamic concepts is, however, used sparingly in this review, most emphasis being placed upon factors affecting the spatial distribution of components in the scale and alloy and the influence of these factors on overall scaling behavior.

Other subjects not considered in detail include the oxidation of alloys of the refractory metals[1-5] and the important application of metallic and nonmetallic coatings in reducing oxidation rates. Most theories are illustrated as though oxygen is the oxidizing gas, although similar principles often hold in sulfur, H_2S, CO_2, H_2O, SO_2, etc.

PRELIMINARY CLASSIFICATION

When an alloy is oxidized, the oxides of the components may be completely miscible, producing an oxide solid solution, or they may be completely or partly immiscible, producing multiphase scales. In the case of partially or completely immiscible oxides, a crude categorization for a range of alloys AB, in which A is the more noble metal and B the less noble metal, is as follows:

(1) A relatively narrow composition range near pure A where AO is produced almost exclusively, at least in the external scale.

(2) A relatively wide composition range near pure B where BO is produced exclusively.

(3) An intermediate composition range where both AO and BO are produced.

In composition ranges (1) and (3) it is often possible to get doping of the major oxides. For example, if AO is produced almost exclusively, small concentrations of B may dissolve in the oxide, even if B is of a different valency to A and BO of different crystallographic type to AO, thereby changing its defect structure and growth rate. Furthermore, in the intermediate composition range, AO and BO may combine to give partial or complete layers of a more complex oxide compound.

Elaboration of this classification, in a somewhat similar manner to that of Moreau and Bénard,[8] permits the subsequent discussion to be seen in the perspective of the entire alloy oxidation scene. Initially, the special case of the exclusive oxidation of one alloy component is considered, before procedure to the more general case where both components oxidize (Fig. 1).

Class I

Only one of the following elements oxidizes under the prevailing conditions, giving BO.

(a) The addition (minor) element B oxidizes under the given conditions:
  (1) Internally, giving BO particles in a matrix of A, e.g., Ag–Si alloys dilute in silicon producing SiO_2 particles in a silver matrix (Fig. 1a). The oxygen pressure in the atmosphere is less than the equilibrium dissociation pressure of AO.
  (2) Exclusively externally, giving a single layer of BO above an alloy matrix depleted in B, e.g., Ag–Si alloys richer in silicon, producing an external SiO_2 layer (Fig. 1b). The oxygen pressure in the atmosphere is again generally less than the dissociation pressure of AO. A special case of this situation exists, however, where both

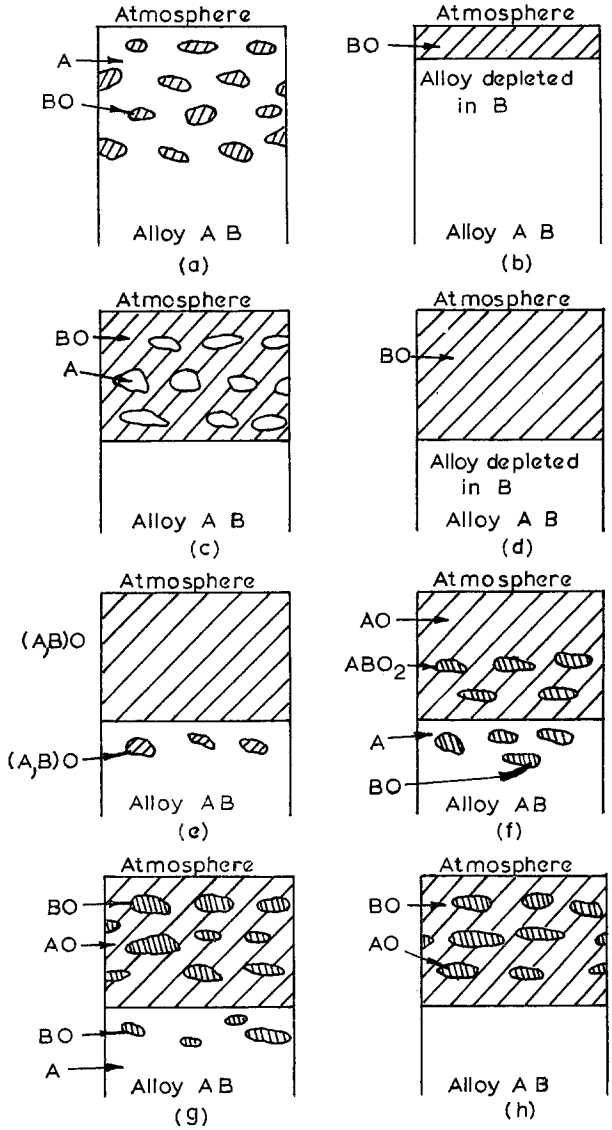

Fig. 1. Schematic representation of modes of oxidation of alloy AB of variable composition, where B is the less noble metal. (a) Minor element B only oxidizes, giving internal oxide BO in matrix of A. (b) Minor element B only oxidizes, giving external oxide BO above alloy depleted in B. (c) Major element B only oxidizes, giving particles of A in a matrix of BO. (d) Major element B only oxidizes, giving external oxide BO above alloy depleted in B. (e) A and B oxidize to give single solid solution or compound of variable composition, (A,B)O. (f) A and B oxidize to give compound ABO_2 dispersed in a matrix of AO. (g) A and minor component B oxidize to give insoluble oxides, with BO in a matrix of AO. (h) A and major component B oxidize to give insoluble oxides, with AO in a matrix of BO.

alloying elements can oxidize but the kinetic and geometrical conditions permit B to be highly selectively oxidized, e.g., Fe–Cr and Ni–Cr alloys reasonably rich in chromium produce essentially Cr_2O_3 scales, especially when oxidized at low partial pressures of oxygen. In practice, small amounts of iron or nickel do enter the Cr_2O_3 scales, producing solid solutions or doping effects.

(b) The element B is now the major element and oxidizes exclusively:
  (1) Leaving the nonoxidizable metal A dispersed in BO, e.g., Cu–Au alloys rich in copper (Fig. 1c).
  (2) Leaving the nonoxidizable metal A in an A-enriched zone beneath the BO scale, e.g., Ni–Pt alloys (Fig. 1d). Fe–Cr alloys richer in chromium than those in Class I(a) (2) come in this category, as do certain Fe–Ni alloys under appropriate conditions.

Class II

Both alloying elements oxidize simultaneously to give AO and BO, the oxygen pressure in the atmosphere being greater than the equilibrium dissociation pressures of both oxides.

(a) AO and BO react to give a compound.
  (1) AO and BO give a single solid solution (A, B)O, e.g., Ni–Co alloys (Fig. 1e). In practice, some internal (A, B)O richer in B than the surface scale is found in the alloy.
  (2) A double oxide is formed, often as a spinel, which may give a complete surface layer of variable composition (Fig. 1e), as for certain Fe–Cr alloys, or particles incorporated into a matrix of AO if the reaction is incomplete, as for certain Ni–Cr alloys (Fig. 1f)

(b) AO and BO are virtually insoluble in each other.
  (1) The less noble metal B is the minor component. An internal oxide of BO lies beneath a mixed layer of AO and BO, e.g., certain Cu–Ni, Cu–Zn, Cu–Al alloys and many other examples (Fig. 1g).
  (2) The less noble metal is the major component so that no internal oxidation is now observed (Fig. 1h). In practice, the second phase in Fig. 1g may not be present in the outer regions of scale because AO may grow rapidly to produce outer regions exclusively of this oxide. The outer regions may be oxidized to higher oxides, e.g., a CuO layer is found outside Cu_2O on Cu–Si alloys. Conditions may develop so that the internal oxide particles link up to give a complete healing layer of BO at the scale base. This can apply to alloys which begin scaling as in Fig. 1g.

It is, therefore, apparent that there is not, and never can be, a single or comprehensive theory of alloy oxidation. Rather, there is a sequence of

special cases. Furthermore, it must be recognized that in certain alloy systems several classifications of behavior are possible, depending on the composition, and oxidation atmosphere, temperature, pressure, time, etc. Changes from one type of behavior to another may occur on a single specimen.

CRITERIA DETERMINING FORMATION OF INTERNAL OR EXTERNAL OXIDATION

The case of alloys AB, such as Ag–In or Ag–Si, in which only one of the components can be oxidized at elevated temperature, is considered first. The component B on the alloy surface produces nuclei of BO in a matrix of A. If B can diffuse up to the alloy surface sufficiently rapidly, a complete surface layer of BO is produced but, if this condition is not met, atomic oxygen diffuses into the alloy, precipitating BO internal oxide particles at appropriate locations. So, the formation of BO internally or externally depends on the balance between the outward flux of B and the inward flux of oxygen in the alloy.

The conditions necessary for the establishment of a complete surface layer of less noble metal oxide, BO, have been discussed in detail by Wagner.[9–12] Assuming the formation of a compact pore-free oxide, the critical concentration of B above which surface oxide BO only is formed is given by:

$$N_B = \frac{V}{z_B M_o} \cdot (\pi k_p / D)^{\frac{1}{2}} \tag{1}$$

where V is the molar volume of the alloy; z_B is the valency of B atoms; M_o is the atomic weight of oxygen; D is the diffusion coefficient of B in the alloy; and k_p is the parabolic rate constant for oxidation.

Moderate or good agreement between theory and practice has been found in specific cases.[12] Under typical conditions in 1 atm O_2, about 10 at.% of B are required to give exclusive surface BO, but this is a rather arbitrary figure, dependent on the alloy and the oxidizing conditions. The value may be reduced to a lower level by reducing the oxygen partial pressure, so-called preferential or selective oxidation conditions. At this critical level of B the volume of precipitated oxide near the surface is so large that atomic oxygen diffusion in the alloy is inhibited by the particles, which eventually coalesce to give a complete barrier to further internal oxidation. The effect of reducing the oxygen pressure is to reduce the flux of oxygen entering the alloy (dependent on both the oxygen solubility and diffusivity in the alloy), without affecting the accompanying flux of B atoms up to the alloy surface. This clearly favors surface oxidation alone at lower B levels in the alloy than are required at higher oxygen pressures.

In alloy systems, AB, where both components oxidize, at high levels of B a virtually pure BO layer is rapidly developed, whereas at lower concentrations BO-rich internal oxide particles are precipitated behind an AO-rich scale. As the oxidation rate slows, however, and the scale layer thickens, conditions in the alloy may change sufficiently to permit the eventual formation of a healing BO layer at the scale base. This situation is discussed in detail later and is termed healing.

Internal oxidation is an interesting subject in its own right but cannot be discussed in detail here. The general subject, with numerous examples, has been well reviewed by Rapp.[12] It has been mainly applied to metals like copper, silver, and nickel with minor additions of silicon, chromium, aluminum, etc., where oxygen diffuses relatively rapidly in the alloy compared with the alloying element. The oxygen level in the alloy is sufficient to precipitate internal oxide particles even when the alloy is covered by the oxide of the more noble metal. The concentration of alloying element B between the internal oxide particles is usually very low if conditions approaching thermodynamic equilibrium are established in the region. Theoretical treatments, providing the rate of penetration of the internal oxide in the presence and absence of an external scale, are available.[12] In certain instances the product of the oxygen diffusivity in the alloy and its mole fraction at the alloy surface can be calculated. One of the most advanced papers on the subject[13] gives a detailed analysis of oxide formation in the internal oxide zone. It is in such studies of the size, number, and separation of particles that future experimental work and theories are most required. It should, of course, be appreciated that internal oxidation can improve or worsen the mechanical properties of an alloy.

THE DISTRIBUTION OF CATIONS IN OXIDE SOLID SOLUTIONS FORMED ON ALLOYS

Figure 2a illustrates schematically the conditions pertaining when a pure metal, nickel, oxidizes to produce a single oxide, NiO, at high temperature, a situation often considered to be the simplest in oxidation theory. NiO is usually considered to be a nonstoichiometric, metal-deficient, *p*-type semiconductor with a virtually perfect anion sublattice but with vacancies on the cation sublattice. Electrical neutrality is maintained by the inclusion of as many Ni^{3+} ions in the nickel sublattice as it contains cation vacancies. Because there is an oxygen pressure or activity difference across the scale, fixed by the equilibrium dissociation pressure of NiO in contact with nickel at the metal–oxide interface, π_{NiO}, and by the ambient atmosphere at the oxide–gas interface, p_{O_2}, there is also an activity or concentration gradient of cation vacancies. The driving force of the reaction is essentially the free

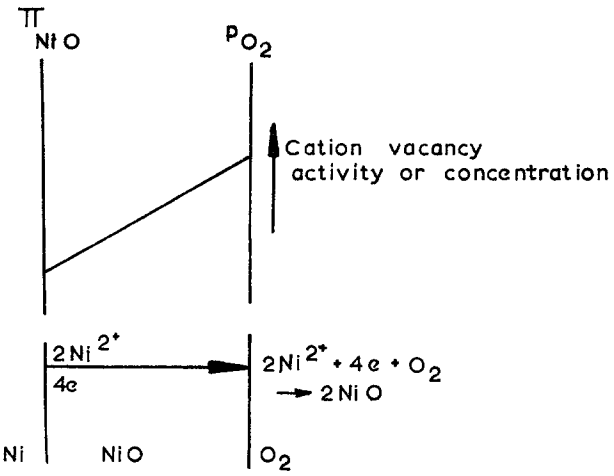

Fig. 2a. Schematic representation of a simple, single-layered NiO scale growing on nickel. P_{O_2} is the oxygen pressure in the atmosphere and π_{NiO} the equilibrium dissociation pressure for NiO in contact with pure nickel.

energy change associated with the oxide formation from metal and oxygen. Reactions at phase boundaries are rapid and it is assumed that thermodynamic equilibrium persists there, so volume diffusion of the reacting ions is rate-determining. With thick scales, neglecting space charge and electrical potential effects, etc., it may be shown that the principal factor controlling growth is diffusion of ions, in this case Ni^{2+}, principally under the existing chemical potential gradient, or vacancy concentration or activity gradient, across the scale. However, the electrical potential gradient is still operative to some extent.

Wagner's classical work[14,15] shows that growth could be expected to follow a parabolic relationship under these conditions. Two processes are necessary to maintain scale growth. Thus, electrons can move rapidly between normal lattice ions (Ni^{2+}) and electron holes (Ni^{3+}) throughout the film to ionize chemisorbed oxygen atoms on the outer scale surface. The cations, which move slower and are rate-determining, diffuse out independently throught the cation vacancies, principally under the vacancy activity gradient, to form fresh oxide at the outer surface. Effectively, cation vacancies are flowing in the opposite direction and must be absorbed by the scale or the metal.

Even this simple, elegant model has been questioned in several respects in recent years:

(1) The lattice defect and electron defect (semiconducting) properties of NiO, and indeed of many oxides, are probably much more complex than

suggested. For example, the number of electron holes ionized or associated with each cation vacancy may be temperature-dependent and the type of defect may also vary with oxygen pressure.[16-18] In the analogous CoO, formed exclusively on cobalt above 900°C, doubly charged cation vacancies may predominate next to the cobalt–CoO interface, i.e., at pressures near the dissociation pressure of CoO, singly charged vacancies at rather higher oxygen pressures and neutral vacancies at pressures nearer 1 atm O_2.[19,20] The complex formation, diffusion, and interaction of these variously charged vacancies through an oxide scale might well influence the oxidation kinetics.[1]

(2) The metallographic observation that scales on nickel and cobalt sometimes appear to contain inner and outer layers[1-5] led to suggestions that the outer layer grew by Ni^{2+} ion diffusion outward and the inner layer by O^{2-} ion diffusion inward through the scale. This latter process seems unlikely, except perhaps down grain boundaries, from considerations of self-diffusion rates of cations and O^{2-} in these oxides[1] and especially as scanning electron microscopy of fracture sections fails to demonstrate pronounced layer structures, but rather reveals a progressive variation in grain size through the scale.[21] It is possibly more likely that some inward oxygen movement occurs in gaseous form through voids, produced by vacancy coalescence and possibly by incomplete plastic flow of the oxide, in the inner regions and perhaps even in the outer regions of the scale. Rapid, short-circuit, gaseous entry from the atmosphere is clearly possible where pores penetrate the entire layer. Where voids are closed, however, they may act as short-circuit paths or as barriers to the ionic diffusion, depending on the circumstances. Oxide nearer the outer surface of the scale has a higher chemical potential than oxide closer to the metal and can dissociate to provide a gaseous supply to build oxide nearer the metal.[22] The question is whether this rate of supply for a given oxide is sufficient to outpace ionic diffusion in the compact parts of the scale in parallel with the voids.[23-25] It is thought that the process can be much more rapid in atmospheres such as H_2O and CO_2, where "carriers" maintain relatively high effective oxygen pressures in the voids.[26] It must also be recognized that at higher temperatures plastic flow of the oxide helps to maintain at least partial contact with the metallic core.

Despite these doubts, the Wagner model provides the basis for considering the general distribution of cations through oxide solid solutions formed on alloys. The simplest case in some respects is (Ni, Co)O growing on Ni–Co alloys, but (Ni, Mn)O growing on Ni–Mn alloys and α(Cr, Fe)$_2O_3$ growing on chromium-rich Fe–Cr alloys are somewhat similar. Wagner has very recently treated the subject theoretically[27] but the equations are relatively so complex, and the assumptions required regarding solid solution

properties and the relative mobilities or diffusion rates of ions in solid solutions as a function of composition are so restrictive, that further consideration from this angle is not pertinent here. When tracer diffusion data are available for the constituent cations in complex oxides, more progress can be made.

At least semiquantitative consideration is more profitably obtained at this stage by measuring concentration profiles in alloy and scale, after various stages of oxidation, using electron probe microanalysis.[28,29] For example, Ni–10.9% Co oxidizes relatively uniformly according to an approximately parabolic growth relationship at 1000°C, giving a scale (Fig. 2b) very similar to that on pure nickel or cobalt, except that there is some internal oxidation. Nickel and cobalt form a continuous range of solid solutions and NiO (a_{NiO} = 4.17 Å) and CoO (a_{CoO} = 4.25 Å) are isomorphous, giving a solid solution of variable composition, (Ni, Co)O. The ionic radii are 0.82 Å for Co^{2+} and 0.78 Å for Ni^{2+}.

The smooth concentration profiles for nickel and cobalt, for a scale produced in 24 hr are shown in Fig. 2c.

The dotted lines near the two interfaces are extrapolations intended to convey the true profiles, masked by x-ray source overlap effects in these locations. As expected, there is a slight depletion of cobalt and enrichment of nickel in the alloy immediately beneath the scale, because cobalt has a marginally greater affinity for oxygen than nickel and is consequently slightly enriched in the steady-state scale. Cobalt diffuses out through the

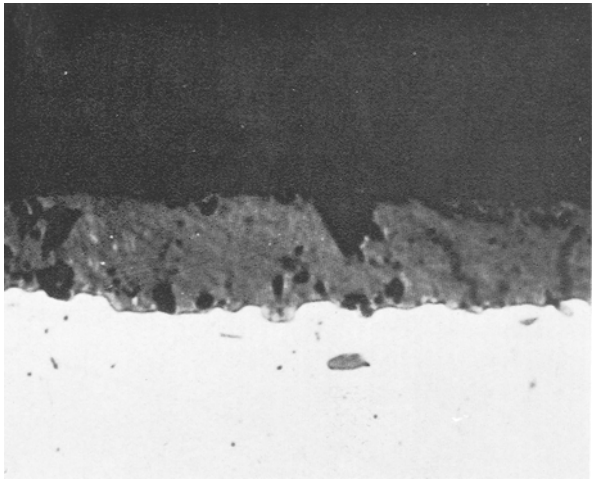

Fig. 2b. Section of Ni–10.9% Co oxidized for 3 hr in oxygen at 1000°C (magnification × 1000). (Courtesy of *Nature*.)

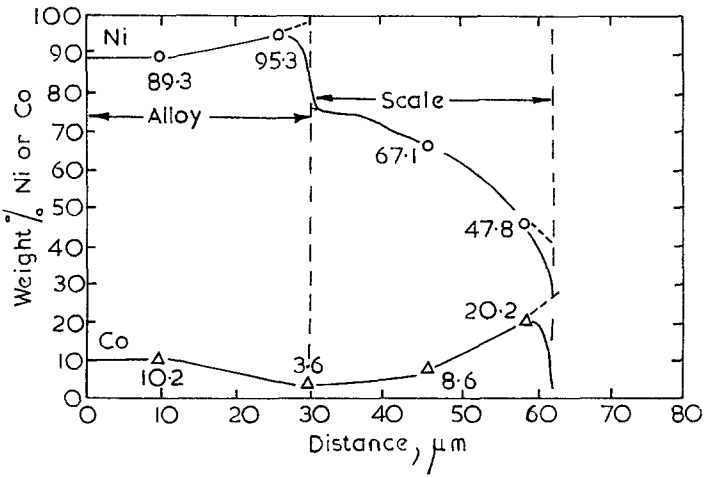

Fig. 2c. Distribution of nickel and cobalt through alloy and scale for Ni–10.9% Co oxidized for 24 hr at 1000°C. (Courtesy of J. M. Ferguson.)

scale faster than nickel, tending to produce the cobalt enrichment at the outer surface. An important observation is that the cobalt and nickel contents in the scale at the alloy–oxide and oxide–oxygen interfaces, respectively, remain constant with oxidation time.[28,29]

Both cations tend to diffuse out through the scale under the influence of the overall cation vacancy concentration or activity gradient, determined largely by the oxygen pressures and concentrations of cations in the scale at the two interfaces, and under the electrical potential gradient,[15] their eventual locations depending significantly on their relative mobilities in this situation. Clearly Co^{2+} has a higher mobility than Ni^{2+}, but the difference does not have to be large to produce the sort of profiles observed.[27,93] Additionally, there is a metal concentration gradient tending to equilibrate the scale composition, by enhancing the diffusion rate of Ni^{2+} and slowing up that of Co^{2+}, but this does not predominate under these conditions. If the scales are subsequently annealed in argon, the metal concentration gradient plays a greater relative role and the scales approach a uniform composition much more closely. The vacancy concentration gradient is reduced for two reasons, namely, the oxygen potential drop across the scale is less, and the metal concentration gradient is also less.

The Ni–Co alloy oxidizes faster than nickel because the rate-determining cation vacancy level at the outside of the scale (in equilibrium with the ambient atmosphere) is greater and probably because the vacancy concentration or activity difference across the scale is greater. It oxidizes at an approximately parabolic rate because the compositions and oxygen

pressures at the scale interfaces, and consequently the corresponding cation vacancy concentrations there, remain constant with time, i.e., the cation vacancy concentration difference across the scale stays constant with time. To a first approximation, the vacancy activity difference must also remain constant, otherwise behavior would not be parabolic. The lack of linearity and other lesser trends in the concentration profiles may be related to the variation in distribution of the charge on vacancies across the scale,[1] to the dependence of the activity coefficient or diffusion coefficient of vacancies on concentration, or possibly to pore formation in the scale. The growth of the outer cobalt enrichment is definite evidence for substantial cation movement during scale growth.

Internal oxidation is possible in this system, presumably because internal oxide, richer in cobalt than the inner surface oxide, can be precipitated in the alloy depths. The cobalt activity is higher in the alloy depths and permits precipitation, whereas some partial dissociation of the oxide is occurring at the alloy–oxide interface where the cobalt activity is lower due to depletion.[28,29] Perhaps impurities, coalesced vacancies, and so forth promote the precipitation. Somewhat analogous precipitation of internal Cu_2O on Cu–Pd alloys with an outer Cu_2O scale has been considered theoretically.[30]

DOPING—THE WAGNER–HAUFFE RULES

The various types of defects in oxides have recently been well described by Kofstad[1] so the treatment is not repeated here. Neglecting the supposedly rare oxides containing substantial numbers of both cation and anion defects, the commonly found nonstoichiometric, semiconducting oxides are normally divided into two general classes:

(1) Oxides with cation defects.
  (a) Metal-deficient, with cation vacancies on the cation sublattice (*p*-type semiconductor), e.g., NiO, CoO, FeO.

or

  (b) Metal-excess, with interstitial cations (*n*-type semiconductor), e.g., possibly ZnO.

(2) Oxides with anion defects.
  (a) Oxygen-deficient with oxygen ion vacancies on the anion sublattice (*n*-type semiconductor), e.g., Nb_2O_5 or Ta_2O_5.

or

  (b) Oxygen-excess, with interstitial oxygen ions (*p*-type semiconductor), e.g., UO_2.

In actuality, the defect structures are often more complex, the oxides containing several types of defects, sometimes linked with impurities.

When a foreign ion or dopant is added to a nonstoichiometric oxide, electroneutrality must be maintained by a redistribution of electronic and ionic defects. For example, with a metal-deficient *p*-type oxide like NiO, addition of trivalent ions such as Cr^{3+} increases the concentration or activity of cation vacancies but decreases the concentration of electron holes. Since transport of cations through the cation vacancies is rate-determining in scale growth, there is an observed increase in oxidation rate. Additions of monovalent ions such as Li^{+} have the reverse effects and reduce the oxidation rate. Comparable rules would apply to oxygen-excess *p*-type semiconductors. For *n*-type oxides of either type, additions of cations of a higher valency than those of the parent oxide decrease the respective concentrations or activities of anion vacancies or cation interstitials, thereby generally reducing the oxidation rate. Lower valency additions increase the oxidation rate. Addition of ions of the same valency should have little effect at such low levels.

The Wagner–Hauffe rules should in principle apply to individual matrix and precipitate phases in multiphase oxides as well as to single-phase oxides, as long as blocking effects of precipitates and certain other general rules regarding the nature of the solution of the dissolving ions are obeyed. The overoptimistic application of the rules has led to disappointment in their lack of generality but closer scrutiny often shows that obedience could not reasonably be expected in real oxidation situations. For the rules to be obeyed, the true defect structure of the parent oxide must be fully understood (many oxides really contain several defects, possibly in association), the foreign cations are assumed to enter normal cation positions in the parent oxide at their anticipated valency, and a Wagner-type parabolic growth relationship must hold rather than a mechanism involving, say, grain-boundary diffusion. Ions often have only limited solubility in the parent oxide, so the rules would not necessarily hold progressively at high addition levels. The ionic radius is a pertinent parameter in such considerations. In ideal cases it is assumed that the dopant is homogeneously distributed through the scale, i.e., the parent and dopant oxidize at the same rate and the rates of diffusion of the two cations in the scale are equal. In practice this probably rarely, if ever, occurs and, except in special circumstances, concentrations of ions at the alloy–oxide and oxide–oxygen interfaces may change with time. Evans[4] has recently summarized cases of obedience and disobedience to the rules.

Even examples which were once considered classical cases of such doping, including the increase in oxidation rate of nickel[23] and cobalt[24] by additions of chromium, are now known to be much more complex. The

increase in oxidation rate is a result of a very subtle interplay of doping, or other alloying effects in the semiconducting oxide, possibly electric field effects, internal and external oxidation, effects on vacancy consumption by the alloy and hence the activity gradient across the scale, pore formation in the inner and possibly the outer regions of the scale, and finally the reduction of cross-sectional area within the scale and at the alloy–oxide interface caused by Cr_2O_3 or $NiCr_2O_4$ or $CoCr_2O_4$ spinel particles.[23,24,31] In one study, doping was dismissed as a minor factor[24] whereas in the other, although the other factors were considered important, the doping was thought, in the initial publication,[23] to be the most likely rate-controlling factor. More recently,[25,31] consideration of the various nickel-base alloys and of dilute Fe–Cr and Co–Cr alloys indicates that the relative importance of the factors may vary from system to system, and the highly complex rather than simple situation is currently being assessed. For example, certain alloy systems show progressive increases in oxidation rate with alloying additions up to 5–10%, whereas in others there is little effect after 1–2% addition. It is undoubtedly evident that internal oxidation makes a bigger contribution to the total weight gain in the Ni–Al system than in the Ni–Cr system.[31,32]

There is insufficient space to elaborate the entire arguments, but examples from the Ni–Cr system are now given and reference is made to the corresponding Co–Cr and Fe–Cr systems. Despite evidence that there is a progressive increase in oxidation rate in oxygen up to 5–8% Cr,[1–5,24] it was found in the study quoted[23,25] that Ni–Cr alloys containing between 1 and 10% Cr at 1000°C, and between 2 and 10% Cr at 1200°C, all oxidize at almost the same parabolic rates but faster than pure nickel. Alloys richer in chromium oxidized slower due to $NiCr_2O_4$ and Cr_2O_3 blocking effects. Figures 3a and b are respectively optical and scanning electron micrographs for sections through typical scales. Figure 3a displays the now well-known morphology of an outer, largely pore-free, columnar-grained NiO zone and an apparently more porous, two-phase, inner region containing $NiCr_2O_4$ in a fine-grained NiO matrix. Cr_2O_3 internal oxide particles penetrate a short distance into the alloy and are converted to $NiCr_2O_4$ upon incorporation into the scale. It is clear how the concept of a compact outer NiO layer and a porous inner layer grew up. However, it must be pointed out that Ni–2% Cr at 1200°C which grew oxide at about the same rate as Ni–5 to 10% Cr had a much less defined demarcation between the two zones. The inner oxide seemed relatively nonporous and contained little $NiCr_2O_4$, as judged by optical microscopy, x-ray diffraction, and electron probe microanalysis. Figure 3b, characteristic of many such scanning micrographs of fractured surfaces, thus avoiding pore enlargement during preparation,[21] shows a *progressive* reduction in oxide grain size from the gas interface to

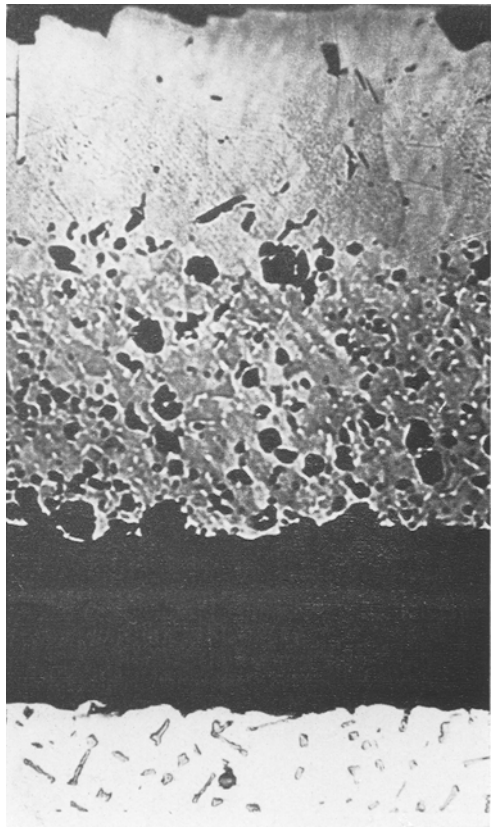

Fig. 3a. Cross section of Ni–5% Cr oxidized for 5 hr in oxygen at 1200°C (magnification × 400). (Courtesy of T. Hodgkiess and I.I.T. Research Institute Symposium.)

the alloy interface. This was true for all alloy compositions. It is by no means evident that a complete porous network exists throughout the inner layer, let alone the entire scale. More detailed scrutiny of the scale regions immediately next to the alloy did suggest a completely porous network there.[21]

Figure 3c gives the nickel and chromium profiles through such a scale, as revealed by electron probe microanalysis. The alloy between the Cr_2O_3 internal oxide contains very little chromium, as expected. The doped NiO between the $NiCr_2O_4$ particles in the inner layer appears to contain 3–4% Cr (compared with 1% at 1000°C) but the chromium level in the outer layer soon declines to a low, scarcely measurable, value ($<0.1\%$). When the

Fig. 3b. Scanning electron micrograph of fractured scale section on Ni–2% Cr oxidized at 1200°C (magnification × 1000). (Courtesy of J. E. Castle and I.I.T. Research Institute Symposium.)

Cr_2O_3 internal oxide particles are incorporated into the scale, they are converted to $NiCr_2O_4$ and tend to saturate the NiO with doping Cr^{3+} ions, any excess $NiCr_2O_4$ then being superfluous. It was also found that, for the alloy ranges mentioned previously, the chromium concentrations in the scale at the alloy–oxide and oxide–gas interfaces were constant at a given temperature for all oxidation times. The measurements are difficult due to x-ray source overlap, fluorescence, smearing, and the low levels being measured. However, they are supported by visual and x-ray examination of the disappearance of precipitate and by hardness measurements in the doped NiO which appeared to indicate a greater solid solution hardening effect for oxide produced at 1200°C than at 1000°C. Scales on the alloys were not as adherent on cooling as those on pure nickel, suggesting that solid solution hardening made the NiO less plastic or affected the vacancy consumption properties of the alloy. Interaction between precipitate particles and the scale may have had some effect.

At the time the preliminary paper was published[23] it appeared plausible to suggest, as in the Ni–Co system, that the cation vacancy concentration or activity difference across the scale would be constant, despite the irregular chromium distribution through the scale, so the same parabolic growth relationship would be obeyed by all the alloys. Although the vacancy

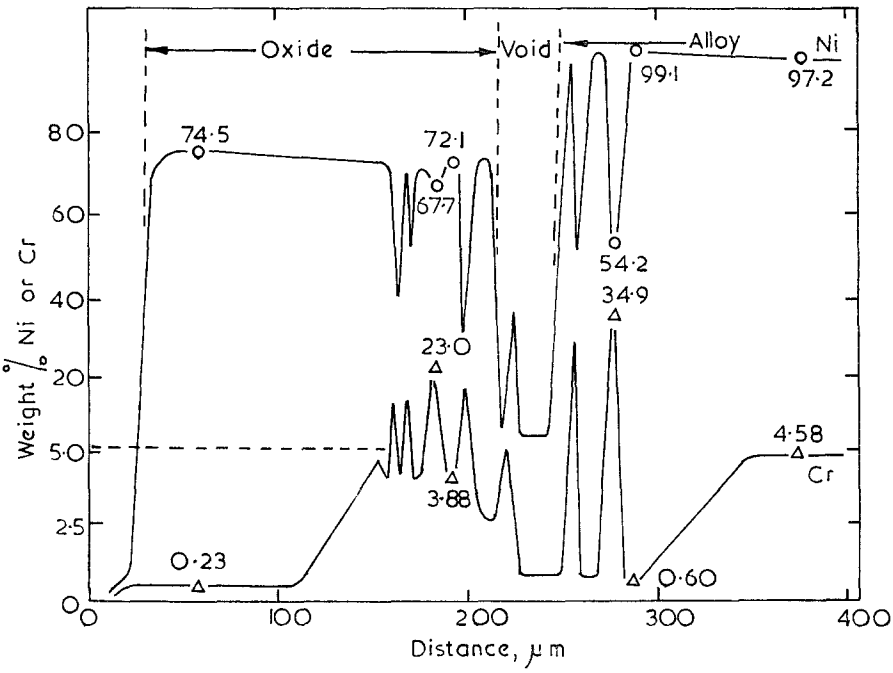

Fig. 3c. Concentration profiles across the scale in Fig. 3a using electron probe microanalysis. Note chromium profile is on expanded ordinate scale. (Courtesy T. Hodgkiess.)

gradient through the scale may be less than for pure NiO, the overall vacancy level and diffusion coefficient in the doped oxide in equilibrium with the ambient atmosphere are greater, so the oxidation rate is increased. This approach is reasonable where only low concentrations of chromium are dissolved in the inner layer. However, at the solubility levels indicated, the cation vacancy concentration gradient would tend to be reversed. It then probably appears more likely that continued growth occurs under the electrical potential gradient alone, arising from electrons tending to hop ahead of the ions via the positive hole mechanism,[27,93] than that the vacancy activity, as opposed to concentration, gradient should still be in the right direction for film thickening, as a result of some defect interaction or association process.[25] It was also indicated[23] that the defect structures of such alloyed oxides are not well understood, that dissociative growth mechanisms in porous inner layers and blocking precipitate effects could be expected, and that possibly the outer layer is rate-determining, the inner layer being effectively short-circuited due to extensive doping or vapor-phase short-circuiting. It did not, however, appear essential to involve these concepts. Other considerations of the Ni–Cr system[33] generally confirm this pattern

but emphasize the role of vacancy coalescence in producing pores in the scale and the alloy.

In a corresponding study of Co–10% Cr[24] is was considered that the outer and especially the inner layers are porous. It was assumed that the rate-determining step is the solid-state diffusion of Co^{2+} ions in the CoO, and possibly in the outer layer only. Gaseous oxygen is rapidly transported across pores, short-circuiting the solid-state diffusion and enhancing the oxidation rate, whereas Cr_2O_3 and the spinel inclusions inhibit oxidation.

Attempts to test for doping in dilute Fe–Cr alloys are soon vitiated by the formation of a rate-determining spinel layer at the scale base and similar layers of pores; nevertheless Fe–0.2% Cr does oxidize faster than iron, due to doping or to the other factors.[31] Recent studies of FeO doped with chromium indicate that the process is highly complex.[34] Thus, neutron diffraction experiments by various workers indicate that pure FeO contains interstitial cations in tetrahedral positions as well as cation vacancies. Adding Cr^{3+} ions to the lattice at the maximum level possible does not appear to cause a big increase in the vacancy level in the oxide in equilibrium with 1 atm oxygen, nor would this be expected. A compensating reduction in vacancies by shifting interstitial iron ions to vacant octahedral cation sites may further offset this effect. However, changes in the ionic bonding and in the configuration of the associated interstitial vacancy complexes may be equally important. The maximum solubility of chromium in FeO seems to be about 2% at 1000°C but its diffusion rate, as in NiO[23,25] and CoO,[24] is low.

Since it would be expected that doping at the concentration levels possible would be more effective in the more nearly naturally stoichiometric oxides, its importance in increasing the cation vacancy level should decrease in the order NiO > CoO > FeO. The likelihood of a cation vacancy concentration gradient reversal also lies in this order. The problem requires further elucidation.

Although reduction in the oxidation rate of chromium and Fe–Cr alloys by lithium addition may be due to doping, it appears that in certain temperature ranges layer formation at the scale base, as with Y-containing alloys, may be a factor.[35,36]

THE APPROACH TOWARD STEADY-STATE SCALING—EFFECT ON SCALE COMPOSITION

Most theoretical treatments,[9,10] and indeed the examples and principles already cited, refer to steady-state scaling. In many systems, however, it requires time and a considerable thickness of scale before the steady-state

pattern is fully set up. The present section considers how the alloy and oxide properties affect this establishment stage, as well as the significant part played by practical factors such as the method of raising the oxidizing sample to temperature, the oxidizing conditions, and the degree of cold work, geometry, and surface finish of the sample. Such factors are particularly important when working near the borderline between "protective" and "nonprotective" behavior, a situation to be expected in practice where materials are being pressed near to their useful limit.

It is usually only possible to predict the equilibrium scale from the thermodynamic considerations, and this may not be the steady-state scale which is sometimes determined by geometrical and spatial considerations. The transient oxides produced when the sample is first exposed often play a major role in determining the nature of the steady-state scale and the subsequent scaling behavior of the alloy.

For fundamental studies, there is no ideal way of exposing the specimen to the atmosphere, especially for alloys rich in aluminum, silicon, and even chromium. There must generally be a surface film of some description on the alloy before exposure to the main atmosphere. If a surface prepared to give a smooth surface, e.g., by electropolishing, is exposed by lowering the sample immediately into the hot zone containing the oxidizing gas, there is always an unsteady heating-up period whose length depends on the specimen and furnace sizes and heat capacities. Considerable oxidation occurs and the scaling pattern is partly established during this heating-up period. On the other hand, if the specimen is brought to temperature in a so-called vacuum (really an oxidizing gas of low oxygen potential for many alloys) before exposure to the main environment, preferential oxidation occurs and unrealistic scaling behavior may be observed subsequently. For example,[37] if Ni–14.6% Cr is immediately exposed to oxygen at 1000°C, a thick stratified scale, similar to that on dilute Ni–Cr alloys, is developed before the eventual steady-state (and in this case equilibrium) doped Cr_2O_3 healing layer is established at its base, eventually giving a low oxidation rate. However, when such an alloy is brought to temperature at 5×10^{-5} torr for 3 hr, before exposure to 1 atm O_2, a thin, relatively adherent doped Cr_2O_3 layer is established from the outset and oxidation is slow for long periods. Similarly, with Ni–40% Cr or Ni–27% Cr, the rather thinner outer NiO layer that is always produced in the scale establishment stages above the doped Cr_2O_3 layer is avoided.

Such preferential oxidation situations are well known in the literature for many alloys.[1–7] If the reverse procedure is employed, namely, the oxygen partial pressure is substantially reduced at some stage during the scaling run, a healing layer of different composition is often produced beneath what had been a rapidly growing steady-state scale at the higher

oxygen pressure. For example,[38] healing NiO or ZnO layers are readily produced by this means at the base of stratified largely Cu_2O-containing scales on Cu–Ni and Cu–Zn alloys respectively.

The industrial equivalent of these situations is related to the heating cycle adopted to bring new equipment into commission, and the reoxidation of "bare alloy" exposed by spalling at temperature or upon thermal cycling. There may be some merit in bringing the equipment to temperature slowly, preferably under a low oxygen partial pressure, to promote the development of a protective layer by preferential oxidation. However, if this layer fails later, protection could be short-lived. Scale spalling at temperature can be the most severe circumstance because "bare alloy," often depleted in the element giving the protective scale, is immediately exposed to the full severity of the atmosphere at its maximum temperature, and rapid, nonprotective scaling may well ensue. The situation is less severe, in some respects, upon thermal cycling because the scale may spall at a lower temperature and there is the possibility of developing a protective layer during the new heating-up period. However, the extent of scale spalling is often more severe during cycling and repeated failure of large areas of scale can be catastrophic. It does not follow that the most protective scale isothermally is the most efficient under cycling conditions. Partial or complete scale adhesion can be as important as the scale composition.

Nucleation in the sense of considering the growth of individual oxide crystals at preferred sites on an alloy surface has been extensively studied and well described.[3] Here, the rapid coalescence of such nuclei to give a complete oxide layer is more pertinent and is demonstrated by consideration of Ni–Cu alloys.[39,40] These alloys are single-phase over the entire composition range but give oxides Cu_2O, CuO, and NiO which are virtually immiscible. Nickel tends to be preferentially oxidized and NiO is the equilibrium scale predicted thermodynamically for most of the composition range. It is also the steady-state matrix scale observed, except for copper-rich alloys, but it is not established immediately, particularly upon direct exposure of the alloy to oxygen at 1 atm pressure.

Figure 4 shows schematically the sequence of events leading up to steady-state scaling for Ni–45% Cu and Ni–90% Cu, upon immediate exposure to 1 atm O_2. Considering Ni–45% Cu first, as both components are initially in contact with oxygen (neglecting the thin air-formed film), both oxidize rapidly to give small Cu_2O and NiO nuclei, respectively. There is little time for diffusion in the alloy or overall enrichment of the scale in nickel. The Cu_2O grows faster than the NiO so it protrudes further into the atmosphere (and also probably into the alloy although this is omitted for simplicity), and eventually overgrows the NiO. Once a complete scale is

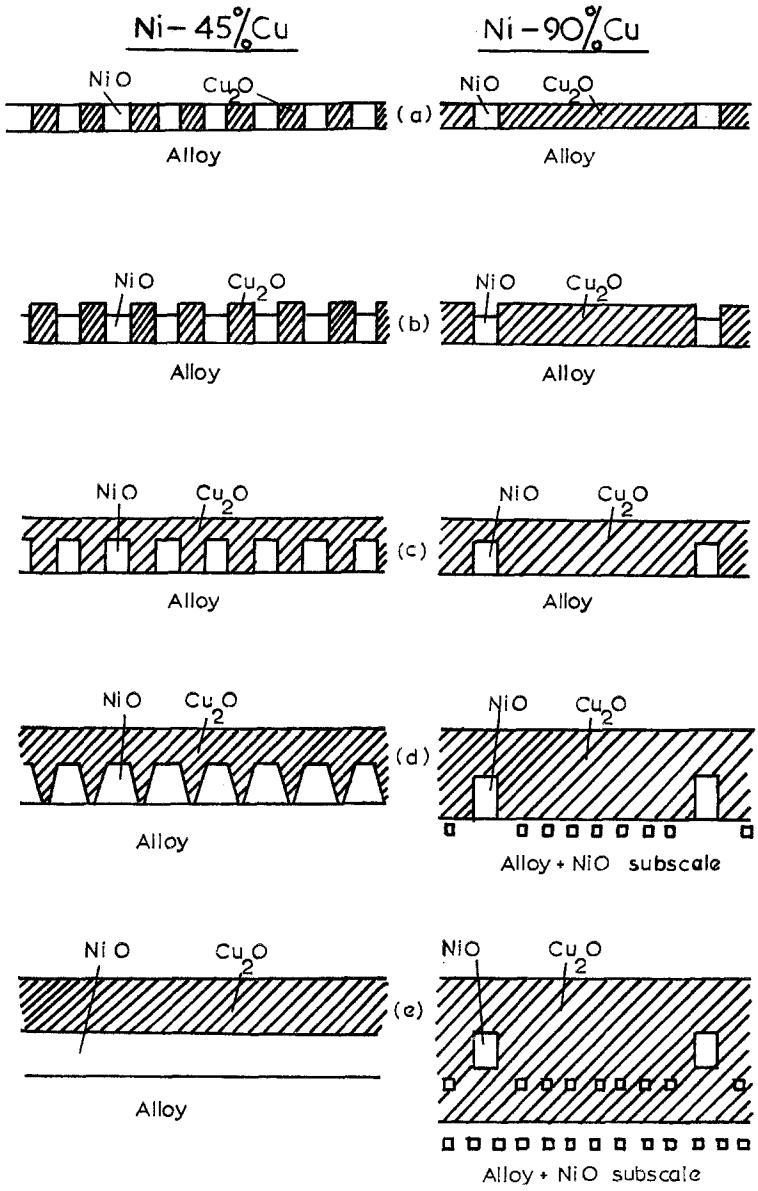

Fig. 4. Schematic representation of approach to steady-state scaling. (Courtesy of *J. Inst. Metals.*)

established, lattice transport of ions becomes rate-determining in the local growth of the coalesced nuclei and diffusion processes in the alloy also play a bigger role. Meanwhile, the NiO is growing laterally as nickel at the

alloy–oxide interface is oxidized directly and also reduces Cu_2O still in contact with the alloy by the so-called "displacement reaction." Eventually the NiO grows laterally to give a complete layer and continues to thicken above for a while, there being very little further copper incorporation into the scale because the effective oxygen pressure at the alloy–oxide interface is less than the dissociation pressure of Cu_2O. The outer copper oxide would only be expected to grow significantly if the Cu^+ ions in the NiO reached a relatively high concentration and diffused very rapidly. This seems more likely in the Ni-Cu-S system.[93,94] The NiO probably oxidizes mainly by the outward diffusion of Ni^{2+} ions, as described earlier, cation vacancies being transmitted across the outer Cu_2O (or CuO as it soon becomes), the outer copper oxide layer thus remaining at constant thickness. As it happens, the subsequent behavior of Ni–45%Cu is rather complex,[40] but the behavior described would apply equally to Ni–20%Cu, and the NiO would continue to thicken indefinitely.

The behavior of Ni–90%Cu is initially similar but the NiO is now never sufficiently abundant to form a complete layer (Fig. 4). Thus, Cu_2O at the alloy–oxide interface can partly dissociate to supply the alloy with atomic oxygen, which diffuses inward, producing a front of internal NiO particles. As the scale thickens, these are incorporated into the inner layer. The inner layer may becomes porous, and it is possible that oxygen gas transport through it is operative, as mentioned in previous sections. The steady-state scaling pattern here is a two-phase surface oxide with a matrix of Cu_2O, and the NiO forming as internal oxide. The equilibrium oxide, NiO, is not produced as a sole surface scale because of spatial and diffusional factors.

Figure 5a shows a transmission electron micrograph of stripped oxide from Ni–45%Cu after 15 sec direct exposure, nominally at 800°C. Although the specimen never reached 800°C, substantial oxidation clearly occurred in this transition period. The micrograph illustrates the initial nuclei, with dark (i.e., thick), acicular Cu_2O particles about 1 μm long and 0.1 μm in diameter protruding from the light (thinner) NiO particles. Naturally, the nuclei are more random in shape than shown in the schematic diagram and have undoubtedly developed in size with exposure time. Soon the copper oxide overgrew the NiO and the scale was too thick for transmission studies. Figure 5b is a plan optical micrograph of Ni–90%Cu oxidized for 10 min at 800°C. The oxide has spalled to display the three layers, namely outer, black CuO which has grown on a reddish-brown Cu_2O layer containing NiO particles incorporated from the alloy, and finally a greenish layer of fine internal oxide particles of NiO in the alloy itself. Full analyses of such relatively thin layers in plan, using electron probe microanalysis, are given elsewhere.[39]

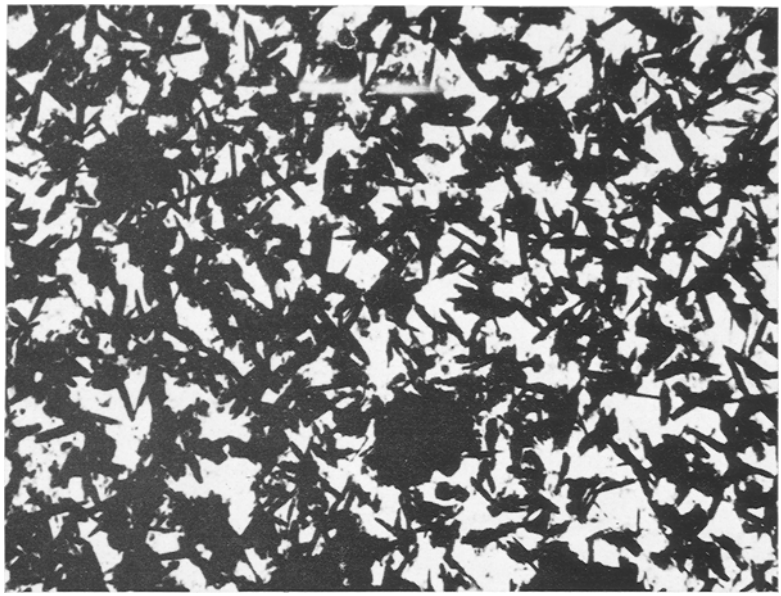

Fig. 5a. Transmission electron micrograph of the oxide film formed on Ni–45% Cu by oxidation for 15 sec in oxygen at 800°C (magnification × 7500). (Courtesy of *J. Inst. Metals.*)

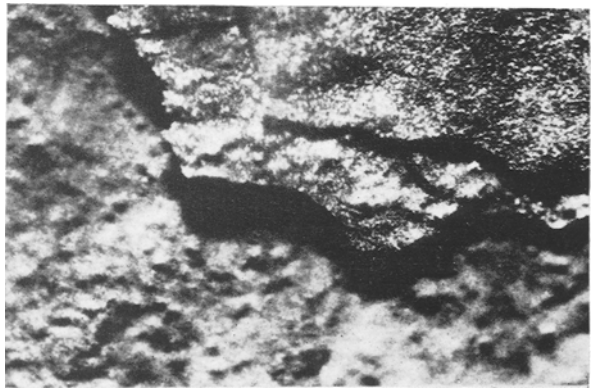

Fig. 5b. Surface topography by optical microscopy of fractured scale produced on Ni–90% Cu after 10 min in oxygen at 800°C (magnification × 80). (Courtesy of *J. Inst. Metals.*)

These considerations enable identification of the important parameters determining how the steady-state scale is established.[9,10,39-43]

(1) The standard free energies of formation of the various possible oxides predict the thermodynamically favored oxide. Preferential oxidation to the oxide with the largest negative free energy value tends to occur. As illustrated, however, this factor is not predominant in the early stages nor does it guarantee the establishment of a complete healing layer of the favored oxide.

(2) The bulk alloy composition determines partly whether there is sufficient favored oxide to give such a healing layer, at least eventually, or whether it appears merely as a nonprotective internal oxide and then as a precipitate in the main scale.

(3) The alloy interdiffusion coefficient determines how rapidly the preferentially oxidizing alloying component can be replenished to any developing surface or healing layer. A high value promotes rapid healing.

(4) The oxygen solubility and diffusivity in the alloy largely determine the internal oxidation characteristics. High values tend to promote internal oxidation.

(5) The growth rates of the component oxides determine the relative development and overgrowth rates of the initial nuclei, and also the rate of scale encroachment into the alloy, absorbing any internal oxide precipitates there before they coalesce into a complete healing layer. The interaction of external scales and incorporated internal oxide particles is also very important in some systems.

(6) The oxidizing conditions, particularly temperature and oxygen partial pressure, as well as the method of elevating the specimen to temperature, are important because they influence all these interrelating factors. Epitaxy effects are only likely to be important at lower temperatures or pressures. For example, when Fe–28% Cr is exposed at 10^{-2} to 10^{-4} torr at 400–950°C, the first oxide formed is the epitaxially related cubic $(Fe, Cr)_3O_4$ or $\gamma(Fe, Cr)_2O_3$. This gradually develops into the usual hexagonal $(Fe, Cr)_2O_3$.[44]

Comparing Cu–26% Zn (typical of Cu–Zn alloys containing more than 20% Zn) and Cu–80% Ni (typical of alloys containing more than 75% Ni), it is clear that there are several reasons why ZnO is more readily established than NiO as the steady-state scale, i.e., the outer copper oxide layer is thinner, for comparable exposure conditions.[39,41,42] The alloy interdiffusion coefficient is several orders of magnitude greater for Cu–Zn than Cu–Ni. This means that there is a great tendency to precipitate ZnO near the surface in the initial nuclei, the flux of zinc outward and oxygen inward

being more nearly matched. Also, the relative growth rates of the doped oxides of copper and zinc are more comparable than those of the doped oxides of copper and nickel, so overgrowth is less prevalent and ZnO can spread laterally more rapidly than NiO to give a complete layer. Finally, zinc has a greater affinity for oxygen than nickel, providing a bigger driving force for the displacement reaction and the direct oxidation of zinc.

Similarly, doped Cr_2O_3 is more readily established initially on Fe–Cr alloys than comparable Ni–Cr alloys[42,43] because of the greater alloy interdiffusion coefficient and smaller oxygen solubility and diffusivity. However, it is less difficult to heal stratified nonprotective scale on Ni–Cr alloys because the nickel-rich oxides grow slower than the iron-rich oxides, thereby giving less scale encroachment on the alloy and absorption of the coalescing internal oxide. Additionally, the oxygen solution characteristics in the Ni–Cr alloys are more favorable to the formation of a dense linking internal oxide layer. Further comparisons for ternary and more complex alloys are given in a later section.

Reduction of the oxygen pressure usually favors preferential oxidation of the component giving the protective oxide, by reducing the oxygen flux into the alloy, leaving the flux of the alloying element up to the surface unaffected. The tendency is, therefore, to precipitate a compact layer near the surface rather than internal oxide. The role of temperature in the establishment of the protective layer has also been considered for Ni–Cr alloys[37] and Ni–Al alloys.[32]

Cold work in an alloy can assist the establishment and maintenance of a protective oxide, not always immediately produced on annealed alloy, by increasing the alloy interdiffusion coefficient,[45,46] but it can also cause spalling of this layer because of residual stresses left in the alloy.[46] If, however, insufficient alloying element is added to give a complete protective layer, cold work may actually increase rather than decrease the oxidation rate, the same matrix oxide being produced as on the annealed alloy. In these circumstances the cold-worked alloy provides an excellent sink for vacancies compared with annealed alloy.[47,48] This maintains a high cation vacancy activity gradient across the scale and prevents void formation by vacancy coalescence at the alloy–oxide interface, thereby permitting a high oxidation rate.

The specimen thickness, geometry, and surface finish are also important but have mainly been investigated for pure metals.[6] The thickness and shape affect the cation vacancy absorption characteristics of the alloy, the heating-up and overheating (due to the heat of oxidation) characteristics as well as the specimen mechanical properties. In addition to controlling the roughness factor, the surface finish often affects the adhesion characteristics

of the scale, more so on Fe–Cr alloys[49–54] than Ni–Cr alloys.[37] Certain finishes may leach alloy components from the surface, whereas in other cases films affecting subsequent oxidation behavior are left on the surface.

STEADY-STATE SCALING—THE SCALE COMPOSITION

Two cases of steady-state scaling have already been considered, namely Ni–Co alloys giving an oxide solid solution and Ni–Cr and Co–Cr alloys giving largely doped oxides which also contain precipitates and pores.[23,24,28] The theory of many other situations has been treated elegantly.[9–11,27,30] Here, several other cases of practical results, relevant to commercial usage, are presented to maintain continuity of argument.

Ni–90% Cu oxidizes very similarly to the dilute Ni–Cr alloys, except that the internal oxide incorporated into the scale remains as NiO, and also an outer CuO layer is produced. Ni–45% Cu oxidizes in the later stages in a complex manner, explicable in terms of the comparable fluxes of metal and oxygen in the alloy.[40] Ni–20% Cu, however, gives a simple scaling pattern. Figure 6a–d shows a typical metallographically prepared scale section and the corresponding electron and x-ray images after oxidation for 100 hr at 800°C. Here the steady-state, dark gray NiO scale has fully established itself and grown thick but the 5–10 μm thick outer light-gray CuO layer should additionally be noted. This grew principally during the scale establishment stages and remained at constant thickness during the continued NiO development. Nickel enrichment in the alloy underlying the scale is evident and confirmed by the microanalysis concentration profiles in Fig. 6e. The small precentages of nickel in the CuO and copper in the NiO could be partly solid solution but there is some evidence of fine particles in other micrographs.[40]

Ni–10–15% Cr at 800–1200°C and Ni–27% Cr at 1200°C act like the dilute Ni–Cr alloys, except they have more $NiCr_2O_4$ in the inner regions of the scale, but become healed by a doped Cr_2O_3 scale in the later stages, especially quickly above grain boundaries.[25,33,37] This doped Cr_2O_3 layer affects the scale plasticity and the ability of vacancies to penetrate to the subjacent alloy.[33] Ni–27% Cr at 800–1000°C and Ni–40% Cr at 800–1200°C oxidize to give doped Cr_2O_3 with an outer NiO layer, rather similar to the behavior of Ni–20% Cu.

However, for reasons given in the previous section, almost pure Cr_2O_3 is developed much more readily on Fe–Cr alloys,[49–54] the outer iron-containing oxide being thin and detected only with difficulty.[55] The scale often lifts off the sample on cooling, principally due to the differential coefficients of contraction of oxide and alloy[49,56] (Fig. 7a). Figure 7b shows that the scale is Cr_2O_3 containing a low level of iron, either doping it or

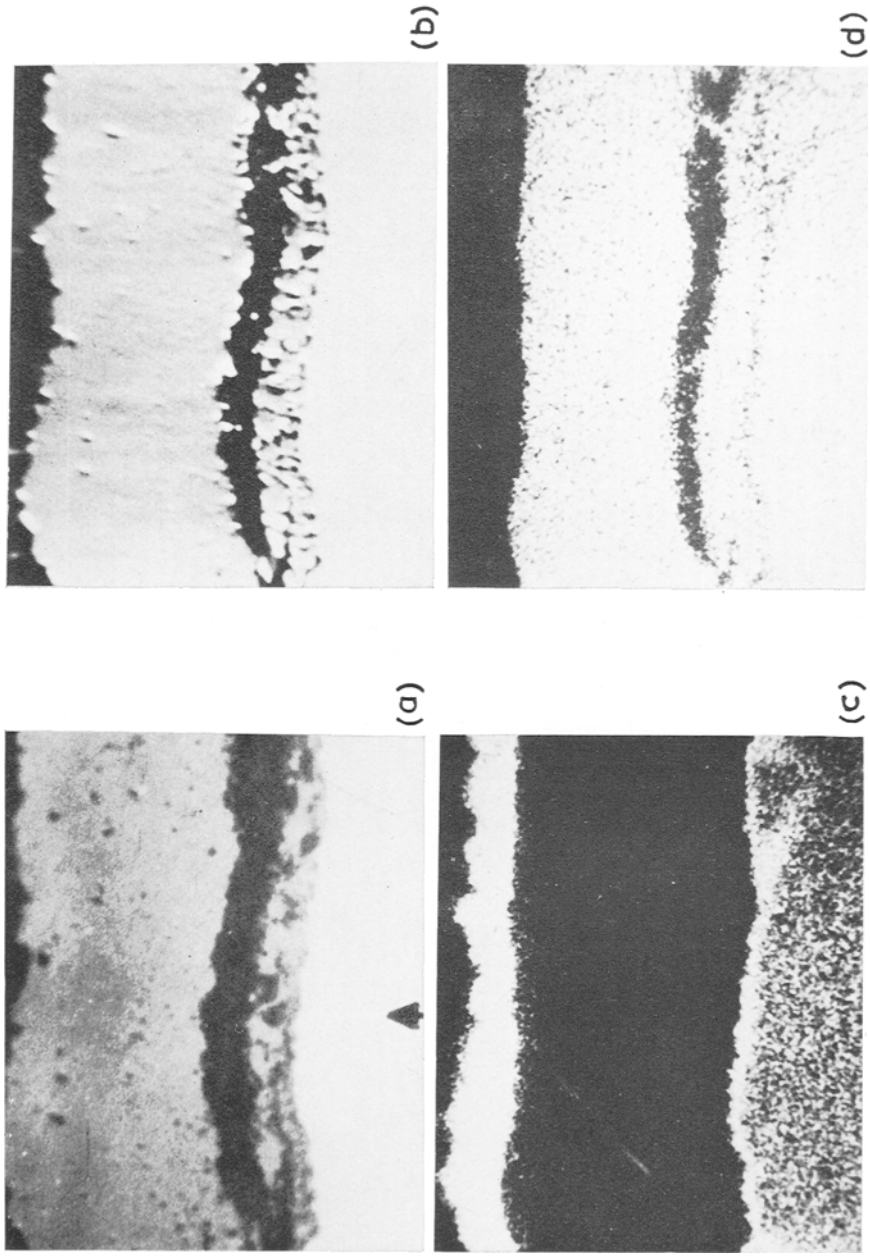

Fig. 6a–d. Cross sections of scales formed on Ni–20% Cu oxidized in oxygen at 800°C for 100 hr (magnification × 1000). (a) Optical. (b) Electron. (c) Cu $K\alpha$. (d) Ni $K\alpha$. (Courtesy of *Corrosion Science*.)

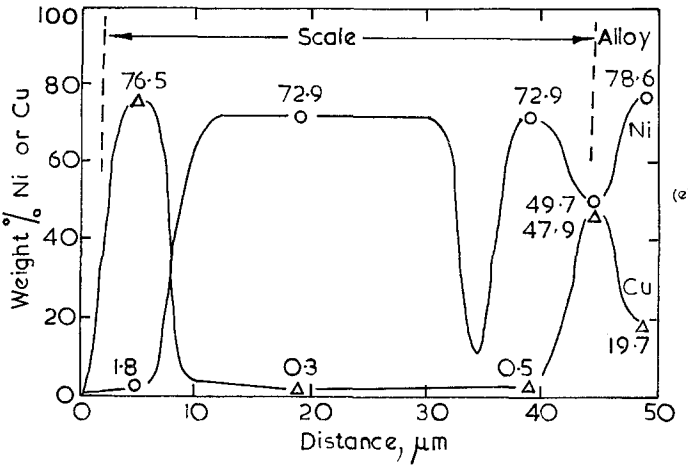

Fig. 6e. Concentration profiles across scale and adjoining alloy shown in Fig. 6a. (Courtesy of *Corrosion Science*.)

present as Cr_2O_3–Fe_2O_3 solid solution. For alloys containing 14–70% Cr, the amount of iron in the bulk Cr_2O_3 is smaller the higher the alloy chromium content, the longer the oxidation time, and the higher the oxidation temperature in the range 800–1200°C. This is because only chromium enters the

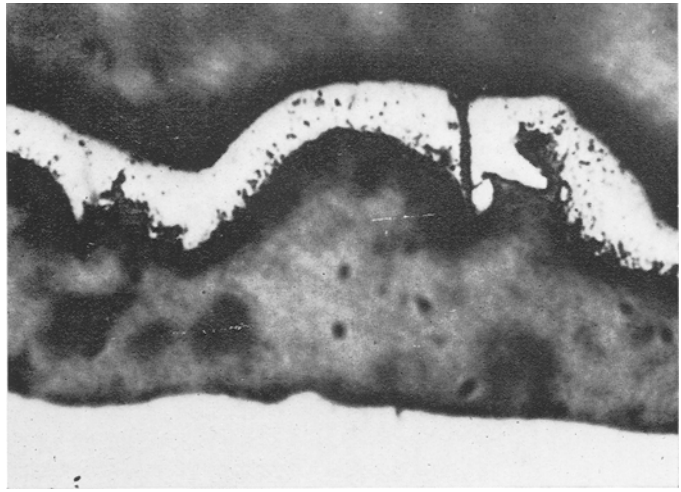

Fig. 7a. Cross section of scale produced on Fe–27.4% Cr after oxidation for 5 hr in oxygen at 1000°C (magnification × 1000).

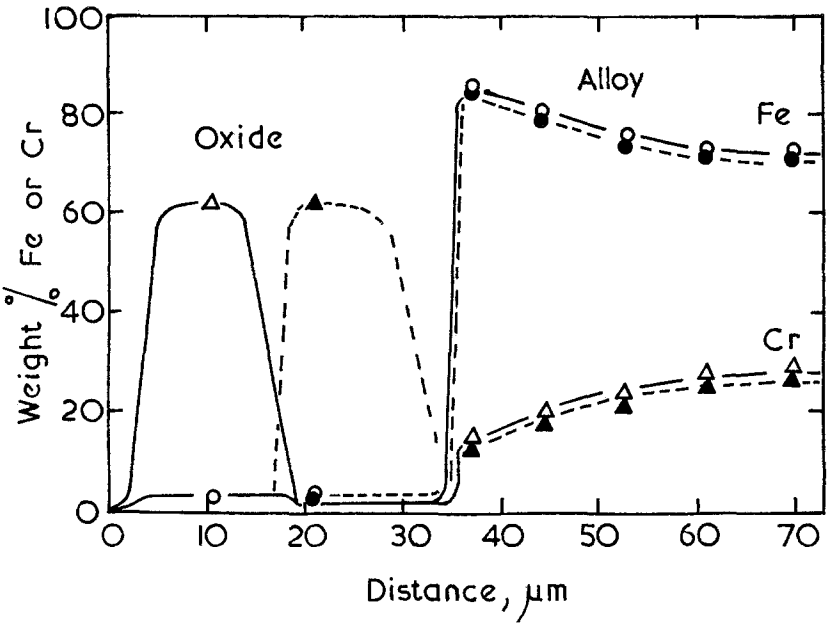

Fig. 7b. Concentration profiles across alloy and scale shown in Fig. 7a. ————Scale detached. – – – – Scale attached. (Courtesy of *J. Electrochem. Soc.*)

scale significantly as the Cr_2O_3 layer thickens and possibly because iron tends to segregate as oxide toward the outer surface (cf. the Ni–Co system). Both the Ni–Cr and Fe–Cr systems display minima in scaling rates at about the 20% Cr level. This could be due to critical doping of the supposedly metal-deficient, *p*-type Cr_2O_3 by Ni^{2+} and Fe^{2+} ions respectively. Furthermore, the effect appears more efficient in the Ni–Cr system. This may mean that part or all of the iron enters Cr_2O_3 as Fe^{3+}, giving essentially Cr_2O_3–Fe_2O_3 solid solution. However, this in itself might be expected to lead to some reduction in scaling because Fe_2O_3 is often recognized to be an anion-deficient *n*-type semiconductor. The minor amounts of nickel and iron within the Cr_2O_3 may also affect its mechanical properties. The underlying alloy depicted in Fig. 7b is depleted from 28 to 14% Cr at the alloy–oxide interface, irrespective of whether the scale was detached or not. The significance of these effects is considered in later sections. In the particular experiments described, volatilization of the Cr_2O_3, probably giving CrO_3, was suppressed by surrounding the oxidizing sample by a crucible containing Cr_2O_3. The volatilization may, however, be treated theoretically, taking into account loss of material to the boundary layer adjacent to the oxide surface.[57]

Other steady-state scaling examples of practical alloys include Fe–Si,[58] Ni–Al,[31,32,59] Fe–Al,[59,60] and Fe–Ni.[61–63] For Fe–Ni alloys, iron is preferentially oxidized, leaving nickel enriched in the underlying alloy. At higher nickel levels, depending on the atmosphere, nickel may enter the scale and a spinel may be rate-determining and the oxidation rate reduced.

THE APPROACH TOWARD STEADY-STATE SCALING—EFFECT ON ALLOY COMPOSITION

It appears that the alloy composition at the alloy–oxide interface takes rather longer than the scale to reach anything approaching steady-state behavior, although it must be recognized that minor changes are probably occurring in the compositions of both alloy and scale long after it seems that the steady state has been reached in the latter. This is because the alloy in contact with the virtually established steady-state scale has to reach a steady value after the scale completion. Furthermore, depletion of the preferentially oxidizing component must still be progressing in the alloy depths because of alloy interdiffusion between the depleted surface layer and the alloy core.

The depletion profile in the underlying alloy for steady-state parabolic scaling, giving complete preferential oxidation to a single surface oxide, has been obtained by analytical solution of the diffusion equations.[9] A finite difference method has been used subsequently to calculate the alloy compositional changes during the approach to the steady state at the alloy–oxide interface for parabolic,[64] cubic,[64] logarithmic,[64] and linear[65] oxidation, and tested for the Fe–Cr system.[66] Assuming that only one of the alloy constituents is oxidized (A in the hypothetical alloy AB—following the nomenclature of the original paper but the reverse of the present paper), the concentration of A at the alloy–oxide interface is mainly dependent on three constants:

(a) The ratio of the oxidation rate constant to the alloy interdiffusion coefficient.
(b) The ratio of the concentration of A in the oxide to that in the bulk alloy.
(c) The ratio of the molecular volume of the oxide to the atomic volume of the alloy (i.e., the Pilling–Bedworth ratio).

Calculations can also be performed where there is a phase change in the alloy and where some time is required to establish the steady-state scale (i.e., where significant scale establishment stages occur).

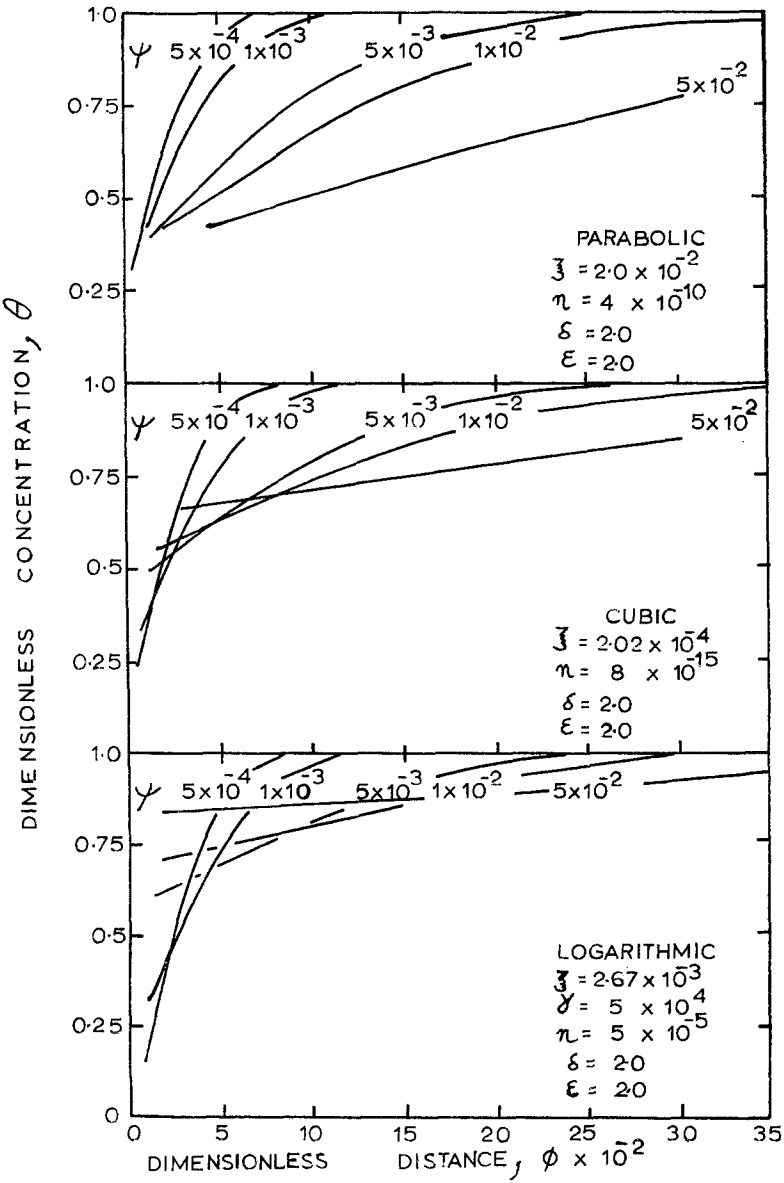

Fig. 8a. Dimensionless concentration of preferentially oxidized element A, θ, as a function of dimensionless distance from the original alloy–oxide interface, ϕ, at various times of oxidation according to parabolic, cubic and logarithmic rate laws.

For increased generality it is appropriate to leave calculated concentration profiles in dimensionless form. Thus, Fig. 8a presents dimensionless concentration against dimensionless distance as a function of dimensionless time for parabolic, cubic, and logarithmic oxidation laws. In essence, the interface concentration starts at a low level and rises progressively with time to a steady value, this being achieved quicker for parabolic than cubic behavior and least rapidly in logarithmic conditions. The depth of penetration of the depletion is a function of the alloy interdiffusion coefficient and oxidation time. For thin sections, it is possible that all, or much of, the entire sample may be affected, with likely serious consequences on the subsequent oxidation resistance and mechanical properties of the sample. For linear oxidation[65] the reverse situation exists, i.e., the interface concentration of the preferentially oxidized component in the alloy drops with time, under the conditions studied.

Although the trends are beyond doubt, it must be appreciated that there is some error in calculating the concentrations in the initial stages. Thus, assuming parabolic growth of AO alone from the outset, the initial oxidation rate would be infinite and the interface concentration of A in the alloy would rapidly drop to zero. However, it is known that true parabolic behavior is not obeyed in the initial scale establishment stages and, as explained earlier, some noble metal would be incorporated into the scale during these stages. Hence, the low value from which the interface value rises with time is unlikely to be zero. It is difficult to pinpoint the value exactly for the above reasons and because of the finite length of the time steps in the analysis.

Figure 8b compares some calculated concentration profiles for the Fe–Cr system with experimentally determined values using electron probe microanalysis. The agreement is within the anticipated experimental error. If the ratio of the oxidation rate constant to the alloy interdiffusion coefficient had been larger, as for certain Ni–Pt alloys,[9] the extent of depletion at the interface would have been bigger. Conversely, it would have been small in a system such as Fe–Al where the ratio is low.[64]

Another quite different case, showing the importance of alloy enrichment and depletion, indicated that the nonuniform accumulation of low melting-point metals beneath scales on mild steel can affect their rolling characteristics.[67]

BREAKAWAY BEHAVIOR

The breakaway of oxides on low alloy steels and zirconium alloys is not considered here. There is, however, considerable evidence regarding the rapid increase in oxidation rate of Fe–Cr alloys, typically in the compos-

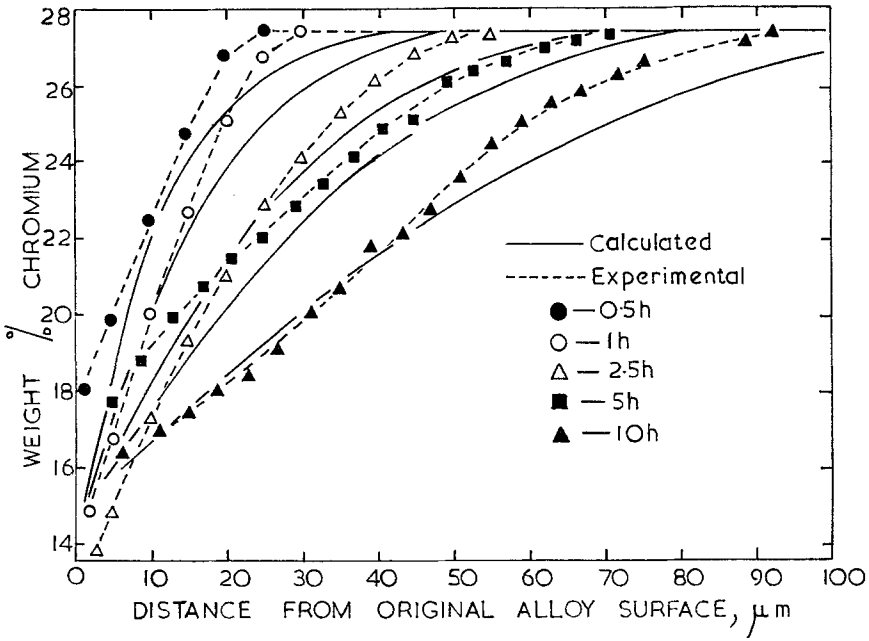

Fig. 8b. Chromium concentration profiles in alloy under scale formed on Fe–27.4% Cr oxidized for various times at 1000°C. (Courtesy of *Acta Met.*)

ition range 14–25% Cr, following an initial protective induction period during which doped Cr_2O_3 scale only is formed. The key to the explanation lies in consideration of the chromium depletion produced in the underlying alloy during the growth of the Cr_2O_3 scale. If the interface value were to fall to a very low value,[66] it might be expected that chemical transformation of the initial scale to an iron-containing oxide would occur.[50,66] This appears unlikely for Fe–Cr-base and Ni–Cr-base alloys, although it might occur with certain alloys and coatings.[66]

All the evidence[49,50] supports a mechanism in which adhesion between the initial doped Cr_2O_3 scale and the underlying alloy is lost, due to stress developed in the system and vacancy coalescence at the alloy–oxide interface, producing ballooning often above grain boundaries[68] and on specimen corners.[50] This must be able to occur virtually isothermally[49,50] but is much more extensive during cooling due to the differential contraction between alloy and oxide.[49,50,68] If the lifted oxide cracks down to the atmosphere, or is removed completely, the chromium-depleted alloy is immediately exposed to the oxidizing gas at high temperature (Fig. 9a). This is a much more severe situation than the more gradual elevation to temperature of the initial sample. The scale establishment stages described earlier are undergone

but in this case the conditions are such as to produce an outer layer containing iron oxide only, an inner layer containing chromium and iron oxides and a chromium-rich internal oxide (Fig. 9b). The iron-rich scale nodule develops rapidly (Fig. 9c) until it may[49] or may not[50] become healed by a new doped Cr_2O_3 layer at its base, by internal oxide coalescence at the scale base. Under fully nonprotective conditions the nodules propagate until the entire specimen surface is covered by stratified scale.

It is generally found that the scale layers in stratified scales in these alloys lie in the order Cr_2O_3, $FeFe_{(2-x)}Cr_xO_4$ ($O \leq x \leq 2$), Fe_2O_3, from the alloy to the outer surface, which is in the order of increasing dissociation pressures as predicted thermodynamically. This is one alloy system where in certain composition ranges, typically 14–18% at 1200°C, a complete spinel layer is produced. It often contains undulating concentration profiles of chromium and iron, for reasons explained in previous publications.[49,50] One further point is that phases produced under these rapid breakaway conditions, and indeed during any initial scale establishment stages, once out of contact with the alloy, are relatively stable even though they are not predicted thermodynamically. They do, however, tend to interdiffuse chemically, producing complex phases or solid solutions.

With Fe–Cr alloys, the likelihood of breakaway is greatest when the surface concentration is low, i.e., in the early stages, but the severity of its continuation is likely to be worse when the depletion has penetrated a considerable distance into the alloy. Clearly, the development of a healing layer is then more difficult. Such breakaway phenomena can occur in corresponding Ni–Cr alloys.[37,43] Potentially, the situation is worse because the chromium depletion at the alloy–oxide interface is greater and longer lasting than for Fe–Cr alloys. In practice, however, isothermal breakaway is rarer because scale adhesion is better, due to a more irregular and interlocked alloy–oxide interface, at least partly caused by the lower alloy interdiffusion coefficient.

INFLUENCE OF TERNARY ADDITIONS TO Fe–Cr, Ni–Cr, AND Co–Cr ALLOYS

Application of the principles already described for binary alloys now permits considerable understanding of ternary alloys and complex industrial materials, at least in relatively simple atmospheres. Frequently, relevant additions and impurities decrease the oxidation rate and improve the scale adhesion. Optimization with respect to trace and minor alloying elements. to produce suitable oxidation resistance, within the restrictions of suitable mechanical properties and cost, provides one of the most promising ways of

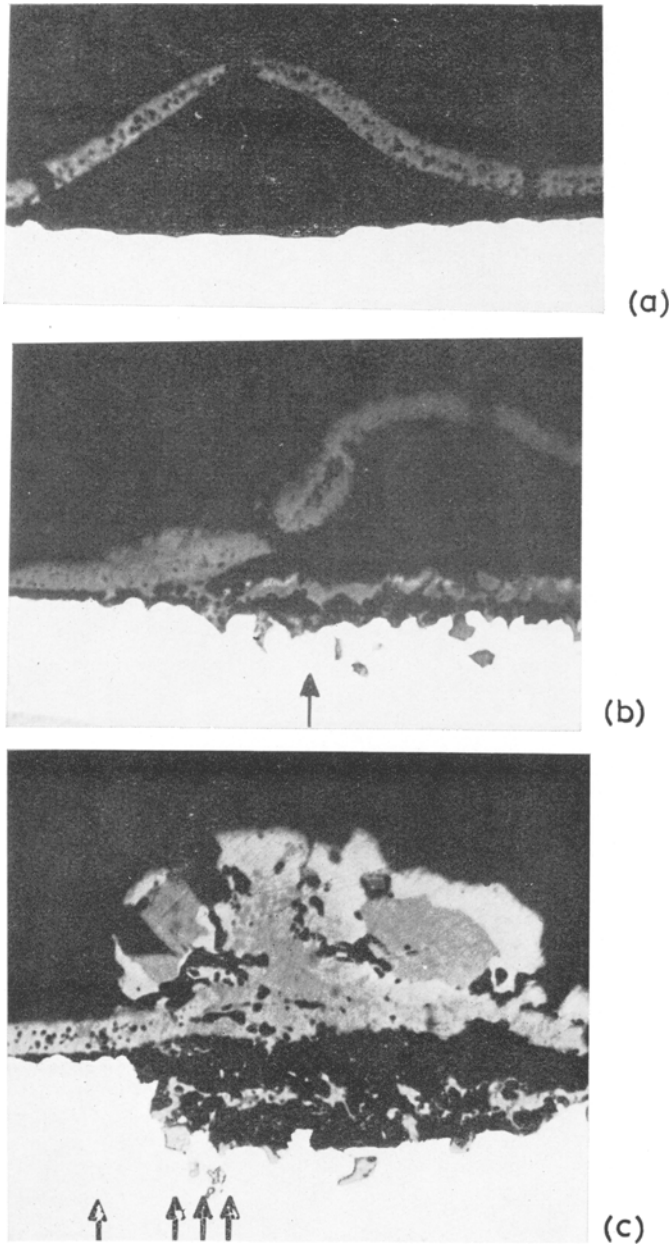

Fig. 9a–c. Cross sections of scales on Fe–14.0% Cr oxidized for 20 min at 1200°C in 1 atm. O_2 after preoxidation, showing breakaway and nodule development (magnification × 500). (Courtesy of *Corrosion Science.*)

developing materials without resort to coatings. Previous advances have usually been empirical but enough is now known about the action of individual elements to make general theoretical predictions. Either available, practical materials may be improved by consideration of how to alter the levels of elements already present[69] or new alloys may be made by specific additions to relatively simple binary or ternary alloys. It should be added, however, that there is still no real substitute for the eventual testing of materials under conditions close to those to be used in practice.

When austenitic Fe–Cr–Ni alloys, based on Fe–28% Cr and Fe–14% Cr, are oxidized in 1 atm O_2 at 800–1200°C, they show certain characteristics of each of the binary systems Ni–Cr, Fe–Cr, and Fe–Ni.[70] Thus, for direct entry to the hot gas, an easily detectable outer layer, which is thick for the alloys based on Fe–14% Cr, is produced before the healing, steady-state, doped Cr_2O_3 layer is established. This outer layer, which contains both iron and nickel oxides, is much thicker than any residual layer found for the Fe–Cr system but, in some circumstances, is thinner than for the Ni–Cr system. In general, the long-term isothermal behavior is better than for Fe–Cr or Ni–Cr alloys. Indeed, the doped Cr_2O_3 thickens slower than on either binary series, presumably because nickel and iron ions dope the Cr_2O_3 more effectively together than singly, and/or because the alloy composition and ability to absorb cation vacancies produces a smaller activity gradient across the scale or voids at its base. The scale adhesion, as on Ni–Cr alloys, is generally good after long times, due to the irregular alloy–oxide interface and possibly to the general specimen mechanical properties. Nonprotective scale development produced by scale lifting is rare isothermally and often produces nickel-rich alloy particles within nodules, similar to those grown on Fe–Ni alloys.[61–63] These nodules in contrast with the smaller ones characteristic of Ni–Cr and even certain Fe–Cr alloys, are not easily healed by a layer of Cr_2O_3 or chromium-rich spinel.

Thus, although nickel has a relatively weak affinity for oxygen, often only entering the scale in relatively small amounts, it plays an important role in dictating the composition, adhesion, and possibly mechanical properties of the protective scale, the severity of its subsequent failure, and its healing characteristics. Attention to the alloy interdiffusion coefficient and the solubility and diffusivity of oxygen in proposed materials, as well as to their bulk composition, should enable better control of these vital characteristics.

Commercial austenitic stainless steels show considerable similarity of behavior to the ternary Fe–Cr–Ni alloys.[70,71] However, other trace elements, such as manganese which is said to give a deleterious nonprotective spinel, and silicon which tends to give intergranular stringers and/or a layer at the scale base slowing the reaction rate, modify the behavior[69,73] Thermal

cycling produces unusual results of interest[74] which require further study by physical methods.

Nimonic 75 shows remarkably similar behavior to Ni–20% Cr upon immediate exposure to oxygen at 1000–1200°C.[25] The weight gain observed before finally establishing the steady-state, doped Cr_2O_3 scale is less than on the binary alloy but the later, apparently parabolic, growth rate is marginally faster. The Cr_2O_3 is apparently doped by manganese, iron, titanium, and silicon as well as nickel, and these elements, except silicon, also appear as successive peaks in the outer, initially nucleated layer. The doped Cr_2O_3 seems better keyed to the alloy on Nimonic 75 than on the binary alloy, there being a more convoluted alloy–oxide interface, and more internal oxide stringers and loops. The chromium concentration at the alloy–oxide interface is higher and the measurable depletion depth greater, suggesting that the alloy interdiffusion coefficient is greater for the commercial material. The other alloying elements follow the anticipated trends. Such alloy interdiffusion effects may be substitutional or a result of more rapid diffusion along numerous subgrain boundaries in the Nimonic 75. These ideas support the observation of a thinner outer layer on the alloy, and would also suggest that isothermal breakaway should be even less of a problem with Nimonic 75 than it is with Ni–20% Cr.

Fe–Cr–Al alloys have interesting oxidation behavior because aluminum competes with chromium in certain composition ranges to give the protective scale. It is well known that it is easier to establish and maintain Al_2O_3 scales on Fe–Cr–Al alloys than on Fe–Al alloys. This may be partly because chromium tends to stabilize α-Al_2O_3 rather than the less protective γ-Al_2O_3.[59] A more general criterion is, however, that chromium reduces the entry of oxygen into the alloy, thereby promoting a complete external layer of Al_2O_3, rather than its precipitation as internal oxide (cf. comparable behavior with Cu–Al and Cu–Zn–Al alloys).[11] This is because Cr_2O_3 and Al_2O_3 predominate over iron oxides in the initially nucleated scale and Cr_2O_3 provides oxygen to the alloy much slower than iron oxides, which have considerably higher dissociation pressures. Consequently, more opportunity is given to the aluminum to diffuse up to the surface and provide the healing Al_2O_3 layer immediately beneath the thin, initially nucleated scale.[11,75,76] It is sometimes claimed that the initial iron oxide and Cr_2O_3 nuclei can be reduced by aluminum in the alloy to give Al_2O_3 by the displacement reaction.[11] While this is in principle true, in practice Cr_2O_3 is usually found outside the Al_2O_3 layer; this is quite reasonable because Cr_2O_3 is stable once out of contact with the alloy, although it does tend to interdiffuse with the Al_2O_3 to give a solid solution.

Although Fe–28% Cr–5% Al gives α-Al_2O_3 scales, with but a trace of residual, initially nucleated, outer Cr_2O_3, Fe–26% Cr–0.9% Al gives

interesting contrasts in borderline behavior, depending on minor changes in conditions.[75,76] Thus, Fig. 10a shows a typical double-layer scale, established upon immediate exposure to 1 atm O_2 at 1200°C, microanalysis indicating that the outer layer is Cr_2O_3-rich and the inner healing layer Al_2O_3-rich. Figure 10b, for nominally identical conditions shows an outer Cr_2O_3 layer containing 0.5–1.5% Al and 0.5–1.5% Fe, but beneath this a banded Al_2O_3-rich internal oxide has penetrated the alloy to a considerable depth. Scale like that in Fig. 10a covered less than 10% of the surfaces of specimens at 1200°C but up to 70% at 1000°C, due to the less severe oxidation. The variations from specimen to specimen and on a given sample are presumably due to minor differences in surface finish, alloy composition, and heating-up characteristics. For the scale in Fig. 10b the Cr_2O_3 could not slow down the rate of oxygen entry into the alloy sufficiently to prevent unabated internal oxidation at a parabolic rate, whereas for the scale in Fig. 10a it just succeeded in doing so, Al_2O_3-rich oxide coalescing to heal the initially grown Cr_2O_3-rich layer. This gave a slow oxidation rate, consistent with the almost stoichiometric, poorly electronically conducting structure of the α-Al_2O_3.

In contrast, samples brought to temperature over 3 hr at 10^{-5}–10^{-6} torr produced a virtually pure α-Al_2O_3 scale, which upon subsequent exposure to 1 atm O_2 thickened slowly over most of the surface (Fig. 10c) for at least 50 hr. The initial preferential oxidation reduces the oxygen flux into the alloy so the Al_2O_3 is precipitated to give a surface layer, which maintains itself and thickens in the more severe atmosphere. Little alloy perturbation in composition is found, or indeed expected, behind Al_2O_3 scales on Fe–Cr–Al alloys because the ratio of the oxidation rate constant to the alloy interdiffusion coefficient is small.[75,76]

Both Cr_2O_3 and Al_2O_3 can balloon at temperature, and more extensively on cooling, on Fe–Cr–Al alloys. For alloys based on Fe–25 to 28% Cr a new Cr_2O_3 or Al_2O_3 layer is usually produced, but for alloys based on Fe–11 to 14% Cr, catastrophic oxidation with severe iron-oxide-containing nodular growths may ensue, even when the aluminum content is considerably higher than 1%.[75,76]

Ni–Cr–Al and Co–Cr–Al alloys give somewhat similar behavior.[31] Preliminary assessment of the results indicates that rather more aluminum is needed to ensure an Al_2O_3-rich scale. Co–Cr–Al is probably the least effective because the alloy interdiffusion rate would be expected to be relatively low and CoO has a rapid overgrowth rate, absorbing the initial Al_2O_3 and Cr_2O_3 nuclei and encroaching rapidly on the developing internal oxide layer. Ni–Cr–Al, although again probably possessing a somewhat lower alloy interdiffusion coefficient than Fe–Cr–Al, is compensated by the low overgrowth and encroachment rate of NiO compared with CoO

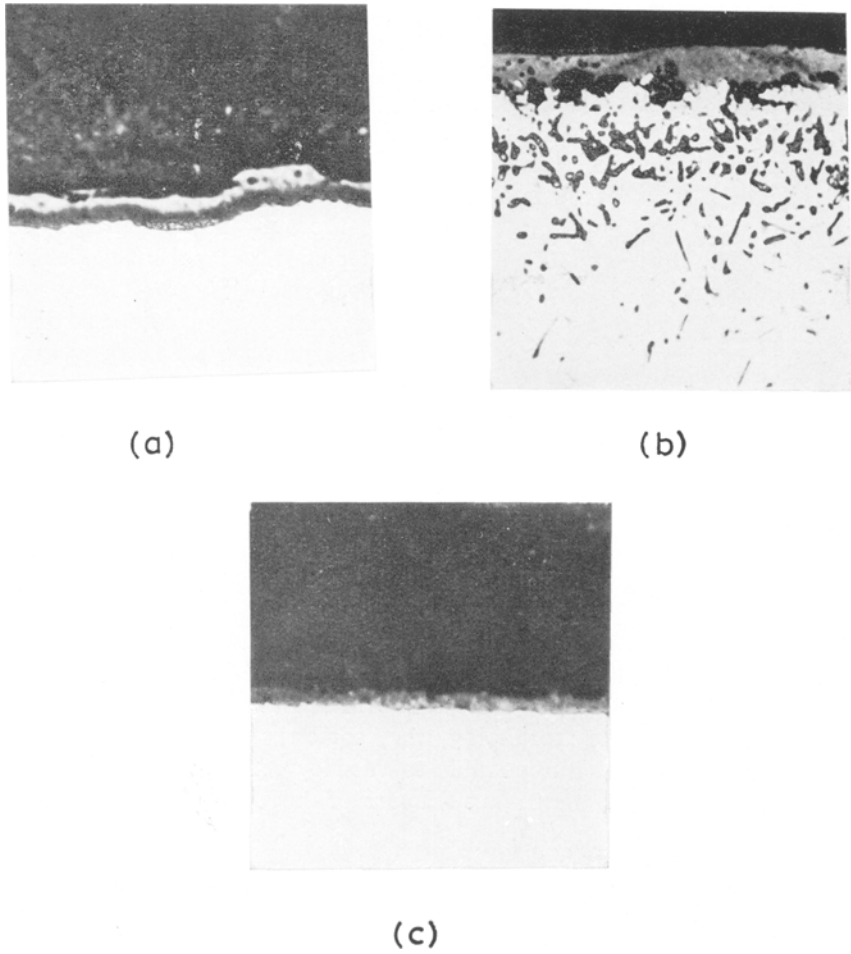

Fig. 10. Cross sections of scales produced on Fe–26% Cr–0.9% Al at 1200°C in 1 atm. O_2. (a) 10 hr (magnification × 750). (b) 10 hr (magnification × 500). (c) 2 hr after elevation to temperature in vacuum over 3 hr (magnification × 1000). (Courtesy of M. G. Hobby.)

or iron oxides. Other factors may, however, contribute to the overall behavior.

Silicon might also be expected to compete with chromium to form a surface SiO_2 layer instead of Cr_2O_3. However, with Fe–26% Cr–1% Si, Fe–29% Cr–5% Si and Fe–14.0% Cr–3.7% Si, it does not succeed, even under preferentially oxidizing conditions.[75] A major reason is that SiO_2 grows so slowly that the initial nuclei are rapidly overgrown by Cr_2O_3,

which continues to thicken until the SiO_2 does manage to pile up at the alloy–oxide interface and spread laterally, providing a healing layer which slows the oxidation rate. This layer may be so thin that it is difficult to detect it in section by optical microscopy or electron probe microanalysis, especially on silicon-rich materials, When it manages to grow slightly thicker, it is visible as a fine particulate, nodular region penetrating slightly into the alloy. Such particulate layers seem to develop from internal SiO_2 behind the Cr_2O_3, barely penetrating into the alloy because the oxygen supply to the alloy and the chromium depletion are both quite small. Silicon-containing intergranular stringers are normally found behind oxides of considerably high dissociation pressure, such as iron oxide. A small silicon level is also measured in the Cr_2O_3 layer but this probably has only secondary effects on the oxidation rate. Although Fe–Cr–Al alloys give a lower weight gain, the eventual scaling rate, once SiO_2 is fully established, appears slower with Fe–Cr–Si alloys. Figure 11a shows the back of a scale stripped from a Fe–Cr–Si alloy, viewed in plan in a scanning electron microscope. The dark phase is Cr_2O_3 and the white, fine-grained layer containing a few cooling cracks is relatively thick SiO_2 (as demonstrated by electron probe microanalysis in plan), developed at its base.[77] Viewing at a glancing angle (Fig. 11b) reveals the SiO_2 linking with the Cr_2O_3 and also the nodular protrusions (about 1 μm in size) into the alloy. Such interface layers clearly affect the scale adhesion characteristics. It should be noted that scales on Fe–Cr–Si alloys are by no means as adherent as those on Fe–Cr–Y alloys, whose morphology they somewhat resemble. The scales are also rather friable, due possibly to vacancy coalescence on the scale above the SiO_2. Thus, the fibrous fracture of the Cr_2O_3 in Fig. 11b may indicate some closed porosity.

It has been known for many years that 1 % or less of rare earth elements in heat-resistant materials improve the isothermal and thermal cycling oxidation performance considerably, especially the vital scale adhesion.[1–5] This is evidently one area where much further work in many circumstances and environments is required. The trace elements may have individual and combined effects and for reasons of expense, and sometimes mechanical properties,[80] the minimum of the cheapest element under the given practical conditions must be estimated. The action may also depend on the main alloy type.

At least under isothermal conditions, there are two distinct effects of Group III A elements, namely reduced scaling rate and improved adhesion.[81] The reduced oxidation rate has been attributed to doping[79] or solid solution effects, but it seems more likely that partial or complete layers of compounds, such as $YCrO_3$ with Fe–Cr–Y alloys, developed at the alloy–oxide interface are responsible,[77–81] as for the corresponding

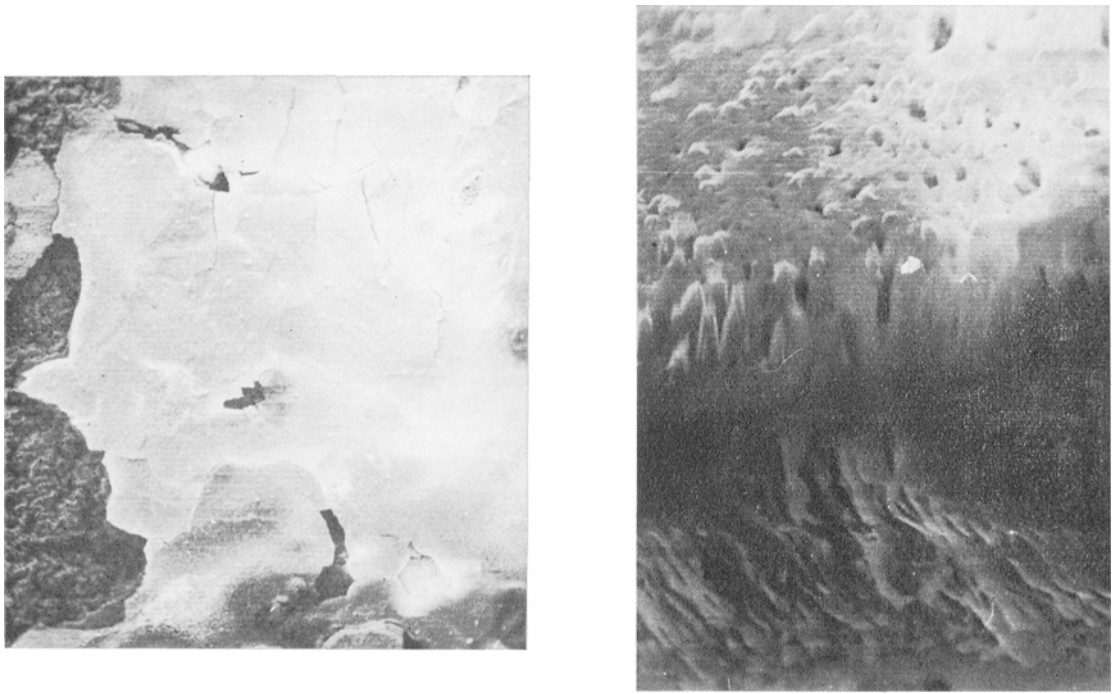

Fig. 11. Scanning electron micrographs of back of scale detached from Fe–14.0% Cr%–3.7% Si after oxidation for 24 hr at 1200°C. (a) Cr_2O_3 (dark) with attached SiO_2 layer (white) showing compactness of SiO_2 except for a few cracks (magnification × 70). (b) Low angle (tilted) view of columnar or granular structure of SiO_2 (top) and fibrous fracture of Cr_2O_3 (bottom) (magnification × 2300). (Courtesy of *Corrosion Science*.)

Fe–Cr–Si case. The asymptotic scaling would certainly support such a mechanism.[81] However, attempts to prove the presence of the layer[77,78,80] are not entirely convincing. Ionic size effects and sintering in the Cr_2O_3 might have some effect but it is not clear how.

The improved adhesion was formerly thought to be due entirely to keying on by tenuous internal oxide but it is evident[77–81] that this is only one, and probably a minor, factor. Other contributions include the slower oxidation rate, the convoluted alloy–oxide interface, the ability of internal oxide particles or the alloy itself to absorb inwardly flowing vacancies, so preventing void formation at the alloy–oxide interface, sintering and the mechanical properties of the alloy–scale composite.[77–81] Under thermal cycling conditions, where continual scale cracking may be significant, the influence of internal oxide and other factors would be particularly important in keeping the grain size small; this would promote metallic diffusion up to the surface (higher alloy interdiffusion coefficient) and help the establishment of a new protective scale. On the other hand, it might be commented that extensive internal oxidation around grain boundaries in these alloys would tend to reduce the flux of chromium up to the surface oxide, rather than increase it.

Further work is also required on the eventual loss of good adhesion, quickly achieved on Fe–Cr–Y alloys at 1300°C and eventually even at 1000°C.[77] Some loss of contact of alloy and scale is definitely produced at temperature, as evidenced by the grain-boundary grooves and faceted alloy grains, related to transport of volatile chromium metal across the void between the alloy and scales.[77] The spalling and opening of the voids may only occur on cooling as no double-layered scales were observed on sectioning the scales.

OTHER ASPECTS AND FUTURE WORK

Some of the areas of current ignorance have been indicated in the previous sections. Here, brief mention is made of aspects of alloy oxidation which have not been covered in the main review and of others where future work is essential.

(1) Coating appears to be the main solution for refractory alloys and other materials with a high solubility for oxygen.[1] Often alloying additions for improved oxidation, e.g., zirconium added to niobium, have to be so large that major changes occur in the oxide structure. However, vanadium and molybdenum additions to niobium alloys may give more compact scales by lowering the oxide melting points, thereby giving increased oxide plasticity and sintering rates.[1] Rhenium additions to Nb–Zr alloys also

lead to a more adherent and less porous external scale, less internal oxidation, and slower oxidation kinetics.[82] Breakaway, and its prevention, for oxidizing zirconium, have been considered in terms of alloying additions.[4] It has been suggested[5] that the volume ratio for oxidation of molybdenum might be reduced by alloying with nickel, for instance, thereby decreasing the stress developed in the oxidizing sample. The influence of alloying on the oxidation of titanium alloys is attributed mainly to the effect of the alloying element on the solution of oxygen in the substrate.[83] These isolated examples represent some of the lines of thought used to improve the oxidation resistance of these alloys.

(2) In principle, the concepts explained in this paper apply to attack in complex gaseous environments, although where deposit attack is prevalent and molten phases tend to destroy the oxide scale, molten salt electrochemistry makes significant contributions. The enormous literature of high-temperature corrosion, much of it consisting simply of factual and semiempirical information, has been considered and reviewed, with some reference to more conventional oxidation studies.[84-86] Minor sulfur contaminants may enter oxide films, increasing the number of lattice defects or lowering the temperature at which softening or partial scale melting occurs. When sulfides themselves are formed, the attack rates are greater than for oxides, because they are much less stoichiometric. Considerable work on attack of alloys by sulfur, SO_2, etc., is now being conducted in various research groups. Principles mentioned for oxidation, such as doping and dissociative growth mechanisms, often seem to hold for sulfidation.[87-89] Oxidation in CO_2-rich atmospheres has been extensively studied in atomic energy technology; behavior is often generally rather similar to that in oxygen, but other factors such as carburization require consideration. Carbon entry into stainless steel[90] and hydrogen movement[92] are examples of the need to measure diffusion of minor reactants. Mass and heat transfer boundary layers may be crucial in deciding the form of product in certain atmospheres and hydrodynamic processes are often vital in deposit attack. In considering complex alloys to combat these various circumstances, the possibility of using combinations of strong and oxidation or corrosion-resistant materials to fabricate plant should not be neglected.

(3) Once the rate-determining layer has been identified, its lattice defect structure and semiconducting properties, including bulk and local diffusion rates must be estimated. Examples of the true complexity of defect structures of simple oxides have been emphasized in this article, and elsewhere.[1] Diffusion rates of major and minor elements in alloy oxides require detailed study, with special attention to the purity levels of the starting materials; ideally these should be oxide layers grown on materials rather than ceramic or "chemically prepared" oxides.

(4) There is so little information on the mechanical properties of oxidizing alloy samples that review is not profitable. Oxides and underlying alloys develop stress because of the dimensional changes upon oxidation, oxygen solution in the metal, nucleation and epitaxy effects, void and layer formation, surface roughness, defect gradients, and so on. At sufficiently high temperatures (but often lower than for bulk oxides) this may be relieved by creep of oxide or alloy, which attempts to maintain contact with the alloy. However, other means of deformation, such as fracture and deformation at high strain rate, may occur isothermally and particularly on cooling or cycling. The cohesion of the oxide and its adhesion to the alloy are obviously important and may be affected by specimen geometry, impact and thermal shock, and mechanical deformation. Differences in the coefficients of contraction on cooling often cause spalling. The hardness of the oxide is important under wear and abrasion conditions.

The various methods available for studying these properties have recently been reviewed in more detail.[6] Here several major points to be borne in mind when planning experiments are listed:

(a) All the properties mentioned are significant in appropriate circumstances; it is important to attempt to define which are the relevant properties for the application in question. Where several factors are involved, they should not necessarily be considered in isolation.

(b) The deforming sample must be considered as a single entity, with full allowance for interactions between the scale and alloy, and geometrical effects. In particular, a considerable ionic flux and also a stoichiometry gradient are present in the scale which should influence certain of the mechanical properties, e.g., creep. Results from bulk ceramics and detached scales, although useful, should be applied with caution. The large flux of vacancies entering the alloy (for metal-deficient, *p*-type oxides) affects the mechanical properties of the alloy.

(c) Many of the methods give average results for the entire specimen. In reality, stress gradients through alloy and scale vary in a complex way. Equally, the alloying constituents are distributed nonuniformly through scales so the local deformation characteristics are important. For example, microhardness measurements indicate how solid solution hardening can vary across thick scales.

(d) Eventually, the mechanical properties must be explained in terms of oxide substructure,[48,92] as has been done so elegantly for metals. The subgrain and dislocation distribution in oxide and subjacent alloy require consideration. Furthermore, direct study by hot-stage electron microscopy will be useful in this respect. Hot stage optical microscopy can also reveal spalling characteristics of thin and thick oxides. The percentage of spalled

oxide may be less important than the properties of the material still adhering to the alloy.

ACKNOWLEDGMENTS

The author wishes to thank Professor T. K. Ross for his support of oxidation work at Manchester and Professor C. Wagner, Dr. D. P. Whittle, and many other colleagues for invaluable discussions.

REFERENCES

1. P. Kofstad, *High-Temperature Oxidation of Metals* (Wiley, New York, 1966).
2. K. Hauffe, *Oxidation of Metals* (Translation from German), (Plenum Press, New York, 1965).
3. J. Bénard, ed., *L'Oxydation des Metaux*, Vols. 1 and 2 (Gauthier-Villars, Paris, 1962 and 1964).
4. U. R. Evans, *The Corrosion and Oxidation of Metals*, Supplement (Arnold, London, 1968).
5. O. Kubaschewski and B. E. Hopkins, *Oxidation of Metals and Alloys*, 2nd ed. (Butterworth, London, 1967).
6. G. C. Wood, in: *Techniques in Metals Research*, Vol. 4, R. A. Rapp, assoc. ed. (Interscience, New York, 1970).
7. G. C. Wood, in: *Reports on the Progress of Applied Chemistry 1968*, Vol. 53 (Society of Chemical Industry, London, 1969), p. 57.
8. J. Moreau and J. Bénard, *L'Oxydation des Metaux*, Vol. 1 (Gauthier-Villars, Paris, 1962), p. 318.
9. C. Wagner, *J. Electrochem. Soc.* **99**, 369 (1952); **103**, 571, 627 (1956).
10. C. Wagner, *Z. Elektrochem.* **63**, 773 (1959).
11. C. Wagner, *Corrosion Sci.* **5**, 751 (1965).
12. R. A. Rapp, *Corrosion* **21**, 382 (1965).
13. G. Bohm and M. Kahlweit, *Acta Met.* **12**, 641 (1964).
14. C. Wagner, *Z. Physik. Chem.* **B21**, 25 (1933).
15. C. Wagner, in: *Atom Movements* (American Society for Metals, Cleveland, Ohio, 1951).
16. W. J. Moore and J. K. Lee, *Trans. Faraday Soc.* **48**, 916 (1952).
17. J. P. Baur, E. S. Bartlett, J. N. Ong, and W. M. Fassell, *J. Electrochem. Soc.* **110**, 185 (1963).
18. K. Fueki and J. B. Wagner, *J. Electrochem. Soc.* **112**, 384 (1965).
19. B. Fisher and D. S. Tannhauser, *J. Electrochem. Soc.* **111**, 1194 (1964).
20. B. Fisher and D. S. Tannhauser, *J. Chem. Phys.* **44**, 1663 (1966).
21. J. E. Castle and G. C. Wood, in: *Proc. Symposium on Scanning Electron Microscopy*, O. Johari, ed. (I.I.T. Research Institute, Chicago, 1968), p. 41.
22. N. Birks and H. Rickert, *J. Inst. Metals* **91**, 308 (1962/63).
23. G. C. Wood and T. Hodgkiess, *Nature* (*London*) **211**, 685 (1966).
24. P. K. Kofstad and A. Z. Hed, *J. Electrochem. Soc.* **116**, 224, 229 (1969).
25. T. Hodgkiess, Ph.D. Thesis, Univ. of Manchester, 1967.
26. C. T. Fujii and R. A. Meussner, *J. Electrochem. Soc.* **110**, 1195 (1963); **111**, 1215 (1964).
27. C. Wagner, *Corrosion Sci.* **9**, 91 (1969).
28. G. C. Wood and J. M. Ferguson, *Nature* (*London*) **208**, 369 (1965).
29. J. M. Ferguson, Ph.D. Thesis, Univ. of Manchester, 1967.
30. C. Wagner, *Corrosion Sci.* **8**, 889 (1968).

31. G. C. Wood, F. H. Stott, and I. G. Wright, unpublished work.
32. F. S. Pettit, *Trans. AIME* **239**, 1296 (1967).
33. D. L. Douglass, *Corrosion Sci.* **8**, 665 (1968).
34. C. T. Fujii and R. A. Meussner, *Trans. AIME* **242**, 1259 (1968).
35. W. C. Hagel, *Trans. Am. Soc. Metals* **56**, 583 (1963).
36. C. S. Tedmon, Jr., *Corrosion Sci.* **7**, 525 (1967).
37. G. C. Wood and T. Hodgkiess, *J. Electrochem. Soc.* **113**, 319 (1966).
38. R. L. Levin and J. B. Wagner, Jr., *J. Electrochem. Soc.* **108**, 954 (1961).
39. D. P. Whittle and G. C. Wood, *J. Inst. Metals* **96**, 115 (1968).
40. D. P. Whittle and G. C. Wood, *Corrosion Sci.* **8**, 295 (1968).
41. D. P. Whittle and G. C. Wood, *Brit. Corrosion J.* **3**, 294 (1968).
42. G. C. Wood, B. Chattopadhyay, and D. P. Whittle, unpublished work.
43. G. C. Wood, T. Hodgkiess, and D. P. Whittle, *Corrosion Sci.* **6**, 129 (1966).
44. V. R. Howes, *Corrosion Sci.* 7, 735 (1967).
45. M. Warzee, M. Maurice, C. Sonnen, J. Waty, and Ph. Berge, *Rev. Met.* **61**, 593 (1964).
46. G. C. Wood and S. I. Ali, unpublished work.
47. D. Caplan and M. Cohen, *Corrosion Sci.* **6**, 321 (1966); **7**, 725 (1967).
48. S. I. Ali and G. C. Wood, *J. Inst. Metals* **97**, 6 (1969).
49. D. P. Whittle and G. C. Wood, *J. Electrochem. Soc.* **114**, 986 (1967); **115**, 126, 133 (1968).
50. G. C. Wood and D. P. Whittle, *Corrosion Sci.* **7**, 763 (1967).
51. D. Caplan and M. Cohen, *J. Electrochem. Soc.* **112**, 471 (1965).
52. D. Caplan, A. Harvey, and M. Cohen, *J. Electrochem. Soc.* **108**, 134 (1961).
53. D. Mortimer and M. L. Post, *Corrosion Sci.* **8**, 499 (1968).
54. D. Mortimer and W. B. A. Sharp, *Brit. Corrosion J.* **3**, 61 (1968).
55. J. Boustead and G. C. Wood, unpublished work.
56. C. S. Tedmon Jr., *J. Electrochem. Soc.* **114**, 788 (1967).
57. C. S. Tedmon Jr., *J. Electrochem. Soc.* **113**, 766 (1966).
58. C. W. Tuck, *Corrosion Sci.* **5**, 631 (1965).
59. W. C. Hagel, *Corrosion* **21**, 316 (1965).
60. F. Saegusa and L. Lee, *Corrosion* **22**, 168 (1966).
61. R. T. Foley, *J. Electrochem. Soc.* **109**, 1202 (1962).
62. I. A. Menzies and W. J. Tomlinson, *J. Iron Steel Inst.* **204**, 1239 (1966).
63. I. A. Menzies and W. J. Tomlinson, *Brit. Corrosion J.* **2**, 235 (1967).
64. D. P. Whittle, D. J. Evans, D. B. Scully, and G. C. Wood, *Acta Met.* **15**, 1421 (1967).
65. D. P. Whittle and G. C. Wood, *Scripta Met.* **1**, 61 (1967).
66. D. P. Whittle, G. C. Wood, D. J. Evans, and D. B. Scully, *Acta Met.* **15**, 1747 (1967).
67. D. A. Melford, *J. Iron Steel Inst.* **200**, 290 (1962).
68. V. R. Howes, *Corrosion Sci.* **8**, 221, 729 (1968).
69. J. M. Francis and W. H. Whitlow, *J. Iron Steel Inst.* **203**, 468 (1965); **204**, 355 (1966).
70. M. G. Hobby and G. C. Wood, *Oxidation of Metals* **1**, 23 (1969).
71. G. C. Wood, M. G. Hobby, and B. Vaszko *J. Iron Steel Inst.* **202**, 685 (1964); **203** 54 (1965).
72. D. Caplan and M. Cohen, *Nature (London)* **205**, 690 (1965).
73. D. Caplan, P. E. Beaubien, and M. Cohen, *Trans. AIME* **233**, 766 (1966).
74. J. M. Francis, C. J. Lee and J. H. Buddery, *J. Iron Steel Inst.* **206**, 921 (1968).
75. M. G. Hobby, M.Sc. Thesis, Univ. of Manchester, 1968.
76. G. C. Wood and M. G. Hobby, *Proc. 3rd Int. Congress on Corrosion, 1966* (Moscow, in press).
77. G. C. Wood, J. A. Richardson, M. G. Hobby, and J. Boustead, *Corrosion Sci.* **9**, 659 (1969).
78. A. U. Seybolt, *Corrosion Sci.* **6**, 263 (1966).
79. J. M. Francis and W. H. Whitlow, *Corrosion Sci.* **5**, 701 (1965).
80. J. E. Antill and K. A. Peakall, *J. Iron Steel Inst.* **205**, 1136 (1967).
81. G. C. Wood and J. Boustead, *Corrosion Sci.* **8**, 719 (1968).
82. R. A. Rapp and G. N. Goldberg, *Trans. AIME* **236**, 1619 (1966).

83. I. A. Menzies and K. N. Strafford, *Corrosion Sci.* **7**, 23 (1967).
84. H. R. Johnson and D. J. Littler, eds., *The Mechanism of Corrosion by Fuel Impurities* (Butterworths, London, 1963).
85. P. Hancock, *Corrosion of Alloys at High Temperatures in Atmospheres Consisting of Fuel Combustion Products and Associated Impurities* (H.M.S.O., London, 1968).
86. D. R. Holmes, *Corrosion Sci.* **8**, 603 (1968).
87. S. Mrowec, T. Werber, and M. Zastawnik, *Corrosion Sci.* **6**, 47 (1966).
88. S. Mrowec, S. Tochowicz, T. Werber, and J. Podhorodecki, *Corrosion Sci.* **7**, 697 (1967).
89. S. Mrowec, T. Werber, and J. Podhorodecki, *Corrosion Sci.* **8**, 815 (1968).
90. W. B. Jepson, J. E. Antill, and J. B. Warburton, *Brit. Corrosion J.* **1**, 15 (1965).
91. P. J. Burkhardt, *J. Electrochem. Soc.* **114**, 196 (1967).
92. G. C. Wood, J. M. Ferguson, B. Vaszko, and D. P. Whittle, *J. Electrochem. Soc.* **114**, 535 (1967).
93. C. Wagner, Private communication; also C. Wagner and K. Zimens, *Acta Chem. Scand.* **1**, 547 (1947).
94. B. D. Lichter and C. Wagner, *J. Electrochem. Soc.* **107**, 168 (1960).